Review

A Review of Photovoltaic Failure and Degradation Mechanisms

Hussain Al Mahdi , Paul G Leahy , Mohammad Alghoul , Alan P. Morrison *

Posted Date: 13 November 2023

doi: 10.20944/preprints202311.0761.v1

Keywords: photovoltaics; reliability; degradation; failure mechanism; solar cells; solar modules

Review

A Review of Photovoltaic Failure and Degradation Mechanisms

Hussain Al Mahdi [1], Paul G. Leahy [2], Mohammad Alghoul [3] and Alan P. Morrison [1]

[1] Electrical & Electronic Engineering, School of Engineering & Architecture, University College Cork, Cork, Ireland.
[2] Energy Engineering, School of Engineering & Architecture, University College Cork, Cork, Ireland
[3] Interdisciplinary Research Centre for Renewable Energy and Power Systems (IRC-REPS), King Fahd University of Petroleum & Minerals, Saudi Arabia.
* Correspondence: a.morrison@ucc.ie

Abstract: With the global increase of photovoltaic (PV) modules deployment in recent years, the need to explore and realize their reported failure mechanisms has become crucial. Despite PV modules being considered reliable devices, failures and extreme degradations often occur. Some degradations and failures can be minor and cause no critical harm if within the expected range. Others, may start mildly and then deteriorate faster to become catastrophic, especially in harsh environments. This paper conducts a state-of-the-art literature review to scan PV failures, types, and their root cause based on PV's constructed components (from protective glass to junction-box). It outlines the hazardous consequences beyond PV module failures, describing what harm they can bring to the PV system. As we delve into the literature, it becomes clear that every component is vulnerable to certain types of failures; some can deteriorate within themselves, and others infect further PV components resulting in emerging more severe failures. In the end, the review briefly summarises PV failure detection techniques, emphasising electrical characterization techniques, and disclosing the need to engage more electrical parameters. Most importantly, this review can prepare the stage for the PV research community to identify the most prevalent degradation processes. This, in turn, encourages researchers to investigate them throughout modelling and experimental studies to forecast them at the early onset in order to protect the PV systems from hazardous malfunctions.

Keywords: photovoltaics; reliability; degradation; failure mechanism; solar cells; solar modules

1. Introduction

Among different renewable energy sources available on earth, solar energy is the most prevalent renewable source in most regions of the world due to its cost-effective applications and installation simplicity [1]. The cost of photovoltaic (PV) systems has declined rapidly over time [2]. Between 1990 and 2020, Germany's PV investment for a 10 kW system dropped substantially by nearly 92.6% from €14000 to €1036 per kW [3]. In the U.S., the decline in the wholesale price for multi-crystalline modules was roughly 95% between 2008 and 2018. Figure 1 shows the average annual addition of solar energy over other renewable energy sources for the past three years.

Preprints (www.preprints.org) | NOT PEER-REVIEWED | Posted: 13 November 2023 doi:10.20944/preprints202311.0761.v1

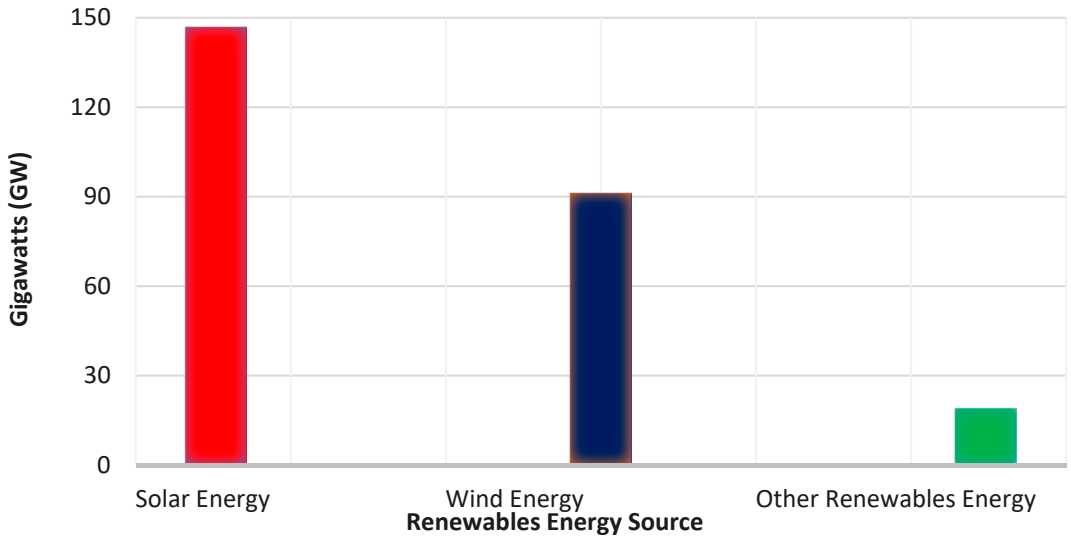

Figure 1. Average annual renewable capacity addition of renewable energy sources between 2020 and 2022[4].

The conversion efficiency of the solar cell has progressed rapidly [5]; nowadays, it converts nearly 26% of the solar spectrum within the wavelength range from 350 nm to 1150 nm into electrical energy [6]. PV cells are serially connected to maximise energy production. Then, they are packaged into modules by the use of a polymer coating, known as the encapsulant, and covered by a protective layer, predominantly made from glass [7,8]. After being encapsulated, the PV module is ready to use and guaranteed by manufacturers to have a 25-year lifetime with an expected degradation rate of 0.8% of power per annum [9–11]. This degradation rate has arrived after many experimental studies and assessments have been conducted. That is, failures found in previously deployed PV modules, such as encapsulant and solar cell defects, prompted the development of these studies. For instance, the National Renewable Energy Laboratory (NREL) developed accelerated stress tests to examine degradation rates, validating the superior quality and long-term reliability of PV modules [12].

1.1. Degradation Rate

A study by Jordan *et al.* [13] examined PV modules that operated for 20 years and found the degradation rate was within the normal range; 0.8% drop in the rated power per annum. However, researchers, e.g., [14–18], agreed that the degradation rate might vary depending on many factors like materials' properties, environmental stress, installation, design and type of connections, and whether the PV system is connected to the electrical grid or standalone. Another study by Jordan *et al.* [19] examined many degradation rates from 40 countries; the findings agreed with [14–17] that these factors significantly affect the degradation rate. It can be spotted from Jordan and Kurtz [32] that the median degradation rate of grid-connected PV systems was higher than stand-alone PV systems deployed in the years before 2000, but became lower after 2000. In addition, these factors were also described by Köntges *et al.* [20], including damage during transportation to degrade the PV module at a faster pace.

Degradation rates of more than 1 % per annum have been reported across deployed PV modules in India [21]. Previous to this, Quansha *et al.* [22] monitored PV modules that operated for 16 years in northern Ghana, particularly off-grid-connected, mono-crystalline type, and found that the annual degradation rate reached 1.54%. The average temperature of north Ghana could reach 30°C, combined with an intermediate humidity level of 43%, which is close to the wither conditions in India. Degradation rates within these ranges represent a double loss in potential power generation than anticipated. Table 1 lists the reported degradation rate of some recent studies.

Preprints (www.preprints.org) | NOT PEER-REVIEWED | Posted: 13 November 2023 doi:10.20944/preprints202311.0761.v1

Table 1 Degradation rate of PV system reported within the last two years.

Degradation Rate	Type of PV (Poly-Si, Mono-Si)	Connection (Grid of Standalone)	Life-Time (Year)	Weather Condition	Country	Ref
Between 0.9% and 1.1%. The rate increased to up to 5.9% with visible failure modes.	Poly-Si	Grid	6	Subtropical climate with moderate humidity level and high temperature.	India	[31]
Modules with no visual defect have around 1% whereas modules with defects may reach 4.2%.	Poly-Si	Grid	10	semi-desert climate, considerably hot and dry weather.	India	[32]
0.6% to 1.2% for modules with no visual defect and 1.4% to 1.9% for modules with defects.	Mono-Si	Standalone	Between 0 to 5	Dry equatorial climate. The average temperature is 28 °C and 30 °C and the average humidity is between 60% and 75%.	Ghana	[33]
0.75% to 1.65% for modules with no visual defect and 1% to 2% for modules with defects.	Poly-Si	Standalone	Between 6 and 10.	Wet semi-equatorial climate. The average temperature ranges between 26 °C and 30 °C and the average humidity is between 70% and 80%.		
The average fluctuates from 0.92% to 1.05%. Modules with defects can reach 3.22%.	Mono-Si	Standalone	10	Hot accompanied by high relative humidity; up to 85.6%	U. S	[34]
1.54% in Mono-Si and 2.72% in Poly-Si.	Both Types	Standalone	11	Dry and hot climate, with frequent sandstorms located in the desert.	Algeria	[35]
The average rate of 20 deployed modules is 1.04%.	Mono-Si	Standalone	11	Warm with a high relative humidity range; the average is 67%.	Algeria	[36]
The average rate of 10 deployed modules is 2.04%.	Poly-Si	Standalone	14	Moderate climate with considerable high relative humidity can reach 83% in the winter months.	Germany	[37]
Between 0.57 and 1.33% based on extracted data and statistical analysis.	Poly-Si	Grid	5	Desert climate, considerably hot and dry. Frequent sandstorms result in dust accumulation on the PV system.	Djibouti	[11]
0.98%	Poly-Si	Not stated	10	Cold and humid, average temperature range between - 6.7 °C and 21°C, average humidity range between 30% and 99%.	Norway	[38] [39]
1.33%	Poly-Si	Not stated	20	PV modules were operated for 10 years in humid and cold weather and then kept inside a research centre for 10 years for examination purposes.		

Furthermore, some PV failures, such as cell cracks, distribute rapidly [33,34]; if undetected, they will cause a significant cost loss that may reach up to 10 fold of the equipment cost [23]. This is because some undetected failures may lead to fire and catastrophic damage to the entire PV system [24]. For instance, critical degradation in some PV modules in an array system leads to mismatch, increasing the PV module's thermal temperature and subsequently leading to fire [25,26]. Critical degradations of PV modules were also listed to initiate fire in a research project based in Germany [24]. Fire can also be caused by hotspot failure, primarily driven by other failure mechanisms that elevate the operated temperature to a hazardous level, and eventually catch fire [27,28]. There have been 80 fire incidents that involved PV in the United Kingdom alone [29]. The fire caused by PV failures is not only resulting in power reduction and cost losses, but it may sadly lead to fatalities; twenty-two casualties related to fire incidents stemming from PV failures were reported in the UK by BRE National Solar Centre [29]. Besides, hydrogen decomposes during PV fires into toxic and life-

 doi:10.20944/preprints202311.0761.v1

threatening gases, namely, hydrogen fluoride and hydrogen chloride [30]. Figure 2 shows a fire incident triggered by a hotspot failure on a module in China.

Figure 2. Fire incident in PV array initiated by hotspot failure [30].

According to Sepanski *et al.* [24], PV modules do not catch fire abruptly; fires are often sparked by critical degradation mechanisms that can be detected in advance.

1.2. Definition of PV Failure

Photovoltaic failure is not defined uniformly in the literature. Some definitions indicate that a drop of 80% in maximum output power is considered a PV failure [40]. Others claim a 20% drop in maximal power is a PV failure [41]. Durand & Bowling [42] defined failure as a drop of more than 50% in maximum power output. However, the International Electrotechnical Commission (IEC) stated the 50% drop in maximum-power output must be accompanied by safety hazards to ascertain failure in the PV module [43]. This discrepancy in defining the term explains the reason for Jordan *et al*. [44] to use the word "degradation mode" instead of "failure" when reviewing the literature. Despite discrepancies in defining the "failure" term, the authors of this paper, use both terms: failure and degradation. The term "failure" is universally described in the literature as any unusual changes in PV modules' appearance, function, and reliability [45,46]. Whereas the term degradation describes the wear-out process of the PV module during its ordinary life cycle. In most cases, the degradation process, if within the expected range, 0.8% drop of rated power per annum, does not harm the PV system unless exceeds this range and moves to a critical phase [38], [46].

In response, this paper reviews the failure and degradation mechanisms of PV module components, providing an awareness of their consequences on safety and power loss in Section 2. Then, briefly scan their classification categories and how they are impacted by environmental stressors in Sections 3 and 4. The review ends by reporting common detection techniques of PV failures and degradation mechanisms. This review, in turn, will assist in ensuring a reliable and safe operation of PV generation and assist the PV community in minimising revenue loss.

2. Failures of the PV Module Components

A PV module consists of solar cells, solders, an encapsulant, protective glass and a back sheet. The raw material of the PV cell comes from element fourteen of the periodic table: silicon. Although silicon is not the ideal element for power conversion efficiency, its semiconductor properties were extensively studied in the market until the development of solar cells [5,47].

Silicon is highly purified and shaped into crystalline perfection and then sliced into a narrow profile ranging between 0.2 to 0.5 mm recognised as a wafer. Residuals of crystalline during the slicing process vary based on the slicing technology. They are frequently used as crystalline ribbons

Preprints (www.preprints.org) | NOT PEER-REVIEWED | Posted: 13 November 2023 doi:10.20944/preprints202311.0761.v1

to reduce manufacturing costs [5]. Once the wafer is connected to the ribbon, the solar cell is ready for testing.

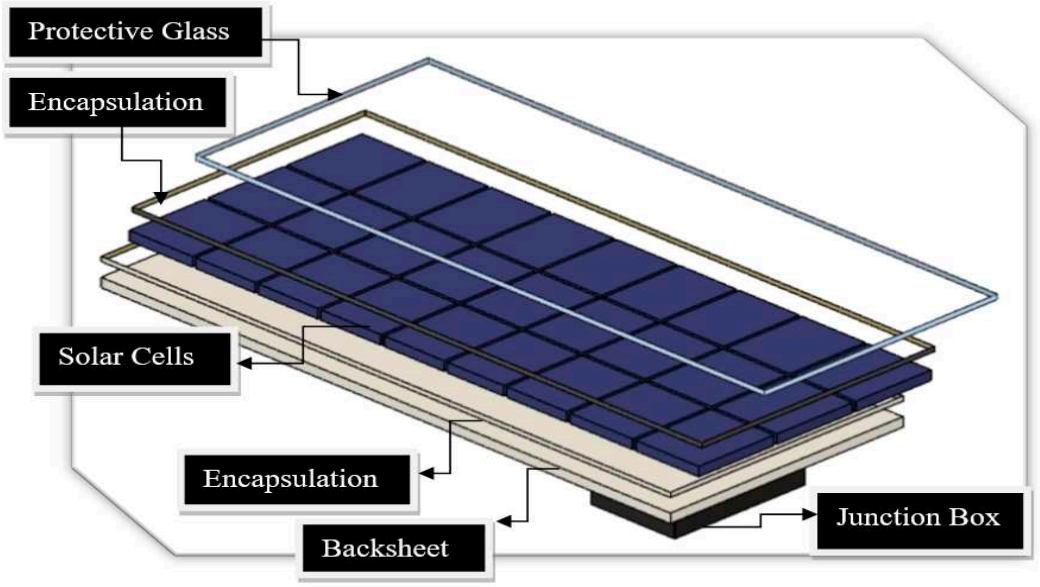

Figure 3. PV module components designed by Fusion 360 modelling program.

2.1. Protective Glass

The protective glass in the PV module is made from tempered glass that consists of a small proportion of iron oxide, not exceeding 0.05%, to allow transmission of sun rays [48]. It is manufactured and designed to resist environmental stress factors such as a drastic shift in temperature.

Gürtürk *et al.* [49] validated glass resistivity by measuring its optical transmittance and energy efficiency. They investigated two types of PV glass, one rated to have a 1% higher solar transmittance. One in each type was used as a control glass and tested at a constant temperature. The others were tested with a drastic shift in their temperature that reached 120°C. Their results showed no significant impact on energy efficiency, only a slight variation, not exceeding 2.06% at most. Afridi *et al.* [50] artificially formed a hotspot via shading with a temperature rising to 200 °C in glass/glass and back-sheet/glass PV modules and proved that the front glass of those two types was not broken or shattered despite severe damage occurring like burn marks, specifically in the glass/glass PV module's type. Belhaouas *et al*. [36] inspected 20 PV modules equipped with two different glasses after 11 years of deployment in Bouzareah, Algeria; eight with float glass and the other twelve with textured glass. Their visual inspection showed more optical failures such as delamination in the float glass types albeit all PV modules suffered from discolouration. Besides, PV modules with float glass type have slighter measured values in the electrical parameters than those with textured glass except for open-circuit voltage. Nonetheless, all twenty PV modules experienced nearly the same degradation rate at 1.04% per year.

Optical reduction of light transmittance is primarily the failure that occurs in PV glasses and is potentially caused by glass breaking or shattering or by harsh weather conditions like ultraviolet rays, and dust accumulation [51,52]. A lab experiment by Tagawa *et al.*[53] explored dust accumulation on glass and its effect on transmittance. Their results revealed a dramatic coarseness increment that resulted in a 32% reduction in glass transmittance after 44 minutes of accumulation. To protect against harmful UV wavelengths, some PV glasses are doped with cerium as an additive [54]. However, King *et al.* [55], discovered, in a laboratory experiment, that doping cerium reduces the optical transmission by 2% in the distant operational period. Kempe *et al*. [56] conducted further experiments on the impact of removing cerium from protective glass and found that exclusive cerium can raise optical transmittance by approximately 1.8% [18], which drives some manufacturers to abandon cerium in production line of PV glass. Alternatively, excluding cerium from PV glass is

Preprints (www.preprints.org) | NOT PEER-REVIEWED | Posted: 13 November 2023 doi:10.20944/preprints202311.0761.v1

extremely risky; it can cause a substantial rise in the rate of delamination failure by a factor of three [56]. Consequently, when it comes to cerium, Kempe *et al.* [56] determined that excluding cerium will not boost electrical efficiency, and if excluded, there is a need to coat the glass with anti-reflective substances to filter out damaging ultraviolet wavelengths, predominantly below 350 nm.

Glass shattering can be the result of poor PV module transportation or incorrect manufacturing processes involving excessive clamping force [15,58–60]. Some weather conditions also participate in PV glass degradation and failures. A study by Bora *et al* [61], analysed failure modes of PV modules in different weather conditions in India, they showed that deployed PV modules in hot areas were vulnerable to glass breakage within five years of operation. Shattering or breakage of the module's glass allows water vapour to ingress the solar cells, creating short circuits and safety risks like electrical shock [32]. This is why glass breakage failure ranked 9 out of 10 in terms of severity as it affects safety severely [32].

In addition, the thermal temperature at the glass's breaking point increases, which may cause hotspot failure [20]. In an investigation study by Chandel *et al.* [62], a PV module found with glass breakage had developed hotspot failures with significant power loss which was also stated by Băjenescu and Titu-Marius [63]. Typically, hotspot forms in a PV module when some cells receive less illumination than others, converting them from energy producers to energy dissipaters, i.e., the energy produced by the fully illuminated solar cells is dissipated by the lesser illuminated ones, increasing the latter cells' thermal temperature and making them operated in reverse bias [64]. Hotspot failures are not only driven by broken glass failures but also driven by shading and mismatch failures [65]. Shading failure is a common PV failure that is strongly linked with hotspot formation [66,67].

When hotspots occur, they cause permanent damage to the solar cells or other module parts; metal connection, EVA encapsulation, or protective glass [68,69]. Jordan *et al.* [44] rated PV failures based on their severity, where one is low, and ten is considered the most severe; they listed hotspots to have the highest severity rate among all PV failures.

However, Ndiaye *et al.* [15] investigated a PV module with broken glass operated for five years and found no hotspot that led to significant power loss. This may indicate that the breaking glass is not the cause of the failure, but the consequences that come afterwards due to weak protection. Bansal *et al.* [32] investigated a PV module operated for 10 years in a mega-plant and found that glass breakage is almost certainly combined with solar cell crack and significant power loss as a result of weak protection.

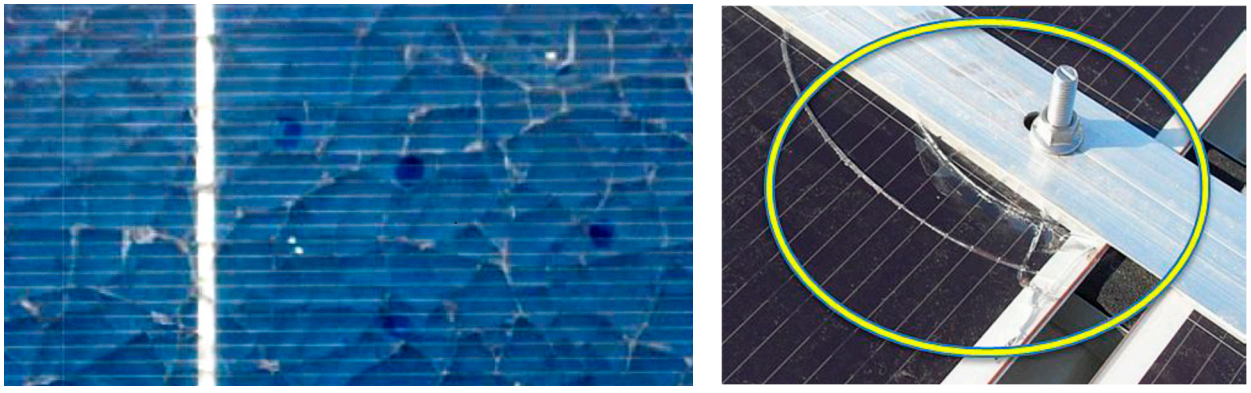

(a) (b)

Figure 4. (a) Example of PV module with a shattered protective glass [57]. (b) Broken glass due to installation fault by too tight bolt [20].

2.2. Encapsulant

Various encapsulating substances have been utilized for photovoltaic modules such as polydimethylsiloxane (PDMS) and thermoplastic polyurethane (TPU) [8,70–72]. Manufacturers

evaluate their advantages and disadvantages in terms of properties including reliability and cost before selection. For instance, PDMS demonstrates better immunity to environmental stress factors which made it favoured in the early stages of PV encapsulation [73]. Recently, manufacturers such as (DuPont) developed a PV encapsulant classified as an Ionomer which offers 25-fold more protection against potential-induced degradation (PID) failure than the typical encapsulant, ethylene-vinyl acetate (EVA). Dow Chemicals, another manufacturer, developed polyolefin-based encapsulants and has claimed it has greater electrical resistance as well as moisture protection when compared to EVA and Ionomers [74,75]. Azam *et al.* [76] explored the degradation rate of four modules: two of which were laminated with polyvinyl butyral (PVB) encapsulant under an accelerated ultraviolet test and found they had a 50% lower degradation rate compared to EVA.

Despite the superior protection features against environmental stress factors in more advanced encapsulating materials, EVA is still utilized in more than 75% of all PV modules due to its cost-effectiveness [77,78]. The cost of PVB material, for instance, is about 50% more per m^2 than its competitor, EVA [76]. The majority of EVA composition is vinyl acetate, with the remainder being a combination of ethylene, antioxidants, and curing agents [79,80].

However, from the historical research carried out in 1981 by Lathrop *et al.* [81] at Clemson University until recent literature reviews, e.g., [82,83], EVA encapsulant is the primary cause of PV degradation mechanisms. Aboagye et *al.*[33] recently inspected polycrystalline and monocrystalline PV modules deployed in three locations in Ghana with different weather conditions, all of which showed defects in EVA encapsulants. The same findings were noted in 43 monocrystalline PV modules mounted for ten years in NORDICS weather conditions, specifically in Grimstad, Norway [38]. Nearly all 43 modules suffered from encapsulant defects, namely delamination or discolouration. In Florida, United States, 156 PV modules were inspected after 10 years of deployment and also revealed the same results as [33,38], all 156 modules exhibited encapsulant delamination failure.

Encapsulant wear out can result in low optical performance in PV modules, which causes a reduction in the electrical output owing to decreased wavelength absorption and extreme light reflection [84]. The encapsulant discolouration effect begins with a drop in the short-circuit current (I_{SC}). The drop in I_{SC} can be as much as 40%, albeit it is not regarded as a PV failure, as it may not pose a safety hazard [43]. Still, discolouration leads to more severe failures like delamination and corrosion, as a result of the release of acetic acid. The released acetic acid in turn is characteristically found responsible for the corrosion of contacts that frequently occurs after the initiation of discolouration failure [85].

With that in context, delamination can cause a substantial decrease in the amount of light absorbed, thereby leading to a significant drop in I_{SC}. Bubble formation is one of the primary triggers of encapsulant delamination; it is formed initially during the lamination process of encapsulation due to a higher localised ratio of released volatile organic compounds [86,87]. The area affected by bubbles in the PV module operates at hotter temperatures and potentially leads to burn marks [88]. A study by Rajput *et al.* [89] analysed the degradation mechanism of 90 mono-crystalline PV modules operated for 22 years in India; it was found that the PV modules affected by more bubbles had more power loss.

Despite ultraviolet radiation occupying a relatively small percentage in the solar spectrum, less than 4%, it is considered a major reason for the degradation of PV encapsulant material [90,91]; due to its shorter wavelength, ultraviolet radiation possesses greater energy that can gradually degrade the encapsulant, decomposing its polymeric bonds [92]. The UV spectrum is divided into three types: ultraviolet type-A, ultraviolet type-B, and ultraviolet type-C. In deployments, PV modules are not exposed to ultraviolet type-C but ultraviolet type-B radiation. Hence, it is regarded as the primary trigger of the degradation mechanism in EVA [93–95]. Even with the implementation of UV-blocking glass, the degradation of EVA remains significant when exposed heavily to UV-B, particularly in conjunction with other stressors such as high temperatures and humidity [56,96]. Consequently, a chemical process is originated, resulting in the creation of acetic acid and aldehyde,

Preprints (www.preprints.org) | NOT PEER-REVIEWED | Posted: 13 November 2023 doi:10.20944/preprints202311.0761.v1

which leads to a gradual darkening of the EVA material from clear to dark brown in severe instances [96,97].

Miller *et al.* [71] examined five types of encapsulants, exploring the degradation process after exposing them to an artificial ultraviolet source and different combination levels of humidity and temperature. Their experiments revealed that encapsulants had higher degradation rates when they were exposed to lower humidity and higher temperatures, displaying faster yellowing. Experiments for exposing PV encapsulant to ultraviolet sources with stressors were also conducted by Arularasu [98] and showed nearly the same results as Miller *et al.* [71].

To account for the degree of encapsulant yellowing, a "yellowing-index" terminology, published by the International Standards Organization (ISO) [99], is used. Yellowing-index is defined as the alteration of polymer colour toward yellow [99]. Nevertheless, Oliveira *et al.* [100] discovered that early degradation of EVA cannot be spotted as it may start before its colour turns yellow, i.e., the yellowing-index has not experienced any modifications. This ambiguity has driven more investigations, for example [54,101,102], to explore the initial stage of EVA degradation.

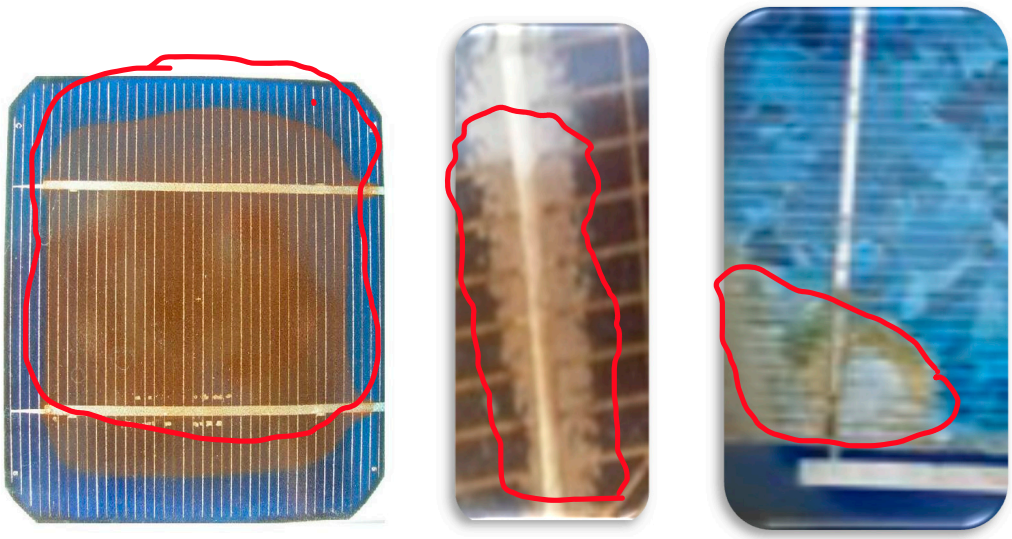

(a) (b) (c)

Figure 5. (A) Brown discolouration of PV cell [103]. (B) PV Module affected by delamination [62]. (C) PV module affected by delamination that led to corrosion [104].

The latter might be the one of reasons for Ferrara and Philipp [105] to state there is no distinct correlation between the shift in the EVA's colour and the solar cell's electrical performance. However, Rosillo and Alonso-Garcia [106] demonstrated through experimentation that an increase in the yellowness index reduces the major electrical parameter, maximum power output. The results of their study are consistent with the well-known research conducted by Pern *et al.* [107], which examined the electrical performance of solar cells for five different colours of EVA (clear, yellow-brown 1, yellow-brown 2, brown, and dark brown). The researchers concluded that as the EVA colour darkened, there was a gradual decrease in the maximum power output, with the most reduction observed in the dark brown colour [99].

In addition, Dechthummarong *et al.* [108] took measurements of PV modules before and after they were mounted for 15 years to ascertain whether the insulation resistance still complied with the IEC 61215 standard [109]. The researchers categorized EVA discolouration into four colours: light yellow, yellow, brown, and dark brown. Their findings revealed that the modules with light yellow and yellow discolouration exhibited healthier performance with superior efficiency when compared to the brown and dark-brown EVA modules. Surprisingly, the insulation resistance of all PV modules met the IEC 61215 standard, even though modules with brown and dark-brown discolouration were more vulnerable to failure from corrosion, delamination, and EVA bubble formation. An

 doi:10.20944/preprints202311.0761.v1

investigation conducted by Diniz *et al.* [110] also found that modules with brown discolouration were associated with more severe and safety-related failures, including corrosion.

2.3. Solar Cells

Solar cells are connected in series and then encapsulated, typically with EVA, to provide adhesion between the solar cells and the protective glass. Failure of the solar cell mainly occurs due to the very narrow profile of the pure silicon slice. These thin wafers are very brittle and are prone to cracking easily during manufacturing or transportation.

Generally, the microcracks of the cell cannot be detected by the naked eye. Due to that, they may spread and distribute to other cells in the module [20]. When the cracks block more than 8% of the cell from functioning, it may lead to a hotspot [20,111]. The active area of the cracked cell may be forced to operate in reverse bias, eventually causing a hotspot failure. Moreover, cracks are subject to expansion and emerging more cracks, especially under environmental and mechanical stress factors like hot, cold, and windy climate conditions [112–115]. Consequently, they accelerate the ageing process, showing a higher degradation rate [20]. Buerhop *et al*. [116] reported that PV modules with cracked cells had a greater than 10% power loss after six years of operation when compared to healthy ones. A study by Siruvuri *et al.* [117] developed a deep learning model based on four attributes; crack type (edge or centre), size, orientation angles (angle degrees of the crack: horizontal vs. vertical cracks) and ambient temperature to forecast the crack severity on power loss. The outcome results were analysed and evaluated, revealing that the power loss increased with increasing crack size and temperature but decreased with increasing orientation angle. However, with regards to angle orientation, their results contradicted the results of *Dhimish et al.* [118], where horizontal cracks are more gentle than those of vertical cracks or so-called parallel to busbar [119].

Conversely, snail track failure can be detected by the naked eye; this failure is so-named because it is shaped like a snail. Alberto *et al.* [120] indicated that most of the snail track failures are linked to the existence of cracked cells. They also compared four PV modules with a snail track against a healthy one. In their findings, the maximum power output dropped in all PV modules with a snail track, one of which had a power loss of 40% than rated. This reduction in maximum power was caused primarily by a significant reduction in the I_{SC}, despite a slight increment in open-circuit voltage (V_{OC}). This association between cracked cells and snail trails was also stressed in a recent investigation study conducted in Indonesia [121]. Duerr *et al*. [122] found that four degradation mechanisms trigger snail track failures, depending on the combination of the encapsulant materials, and on that basis, snail tracks should be described and categorised under PV failures rather than a single degradation mechanism.

Potential induced degradation (PID) is another PV failure observed first in Germany in 2005 [123]. It degrades PV wafers and leads to the development of hotspots [124,125]. It is formed owing to polarization differences between the PV module frame and the module's cells. Thus, it mostly occurs in PV plants and farms where PV frames are grounded as a protective technique against fire ignition [126]. If undetected, it may lead to 100% power loss within a few years [51]. A report based in Germany stated that PID failure is progressing rapidly with the release of acetic acid due to EVA discolouration [127]. Moreover, in a lab experiment by Pingel *et al.* [128], the PV module was found unlikely to recover from PID when operated at higher temperatures. With the rise of bifacial PV module deployment in the last decade, Molto *et al.* [129], reviewed the PID failure displayed in these module types. Although bifacial modules recently joined the PV market, over 30 scientific papers were published in the literature for such failure. The review analysis of Molto *et al.* [129], came with four classifications of PID failures; PID-s, Na-penetration-PID, PID-p and PID-c. Both PID-s and Na-Penetration were caused by the leaning and movement of Na- Na-positive ions to the polarized cells. Involvement of Na^+ ions were also found in PID-c type which was also classified into three categories, whereas PID-p was related to the deterioration of the PV surface. Recovery of all types was found to be possible either fully or partially via dark storage or ultra-violet lighting, particularly for PID-p, but found irreparable for the PID-c type [129].

Preprints (www.preprints.org) | NOT PEER-REVIEWED | Posted: 13 November 2023 doi:10.20944/preprints202311.0761.v1

Another failure that solar cells might experience is a disconnection of the solar cell wires known as busbars or ribbons. This type of failure occurs because of a manufacturing defect, it is also driven by excessive heat due to long partial shading. it can produce excessive leakage current. When undetected increases the thermal temperature and forms a hotspot [130]. Such failure is detected by an infrared camera (IR) or by monitoring the output *I-V* curve. When this occurs, the power is dropped by 35%. With progression, it will decrease the power by 46% [33]. Consequently, the solder bound will become extremely hot, leading to burning marks and discolouration of the EVA encapsulant [131]. In the worst scenario, the protective glass will be broken with visible burn marks on the PV module's back sheet, blocking the current path and initiating an electrical arc and fire, causing irreversible damage [20].

Colvin *et al.*[132], explored interconnection failures depending on cut location in the PV module and irradiance. They investigated cuts in busbars that connect cells in the centre of the PV module and cuts in outer busbars (at the edge). Results showed that outer busbars' cuts are more severe and reduced modules' power output by nearly double compared to those cuts in centred busbars. They justified their findings as alternative busbars that can carry the captured photocurrents are limited to one when cuts occur at the outer busbar, whereas in inner cuts there is more than one alternative busbar that can act in place. Eslami *et al.* [133], explored failures immunity in three common interconnections types in PV modules through FEM simulation; the first one is the conventional interconnection known as front-to-back interconnection, the second type is the light-capturing type which is named due to recapturing of lost photocurrent via reflection; the third type is the multi-busbar which uses its rounder shape effect to reflect the lost photo-currents to cell. Among the three, the multi-busbar type showed 15 per cent higher immunity against ribbon and busbar failures.

Thus, as with most PV failures, detecting them earlier is essential to assure a reliable and safe operation of the PV system.

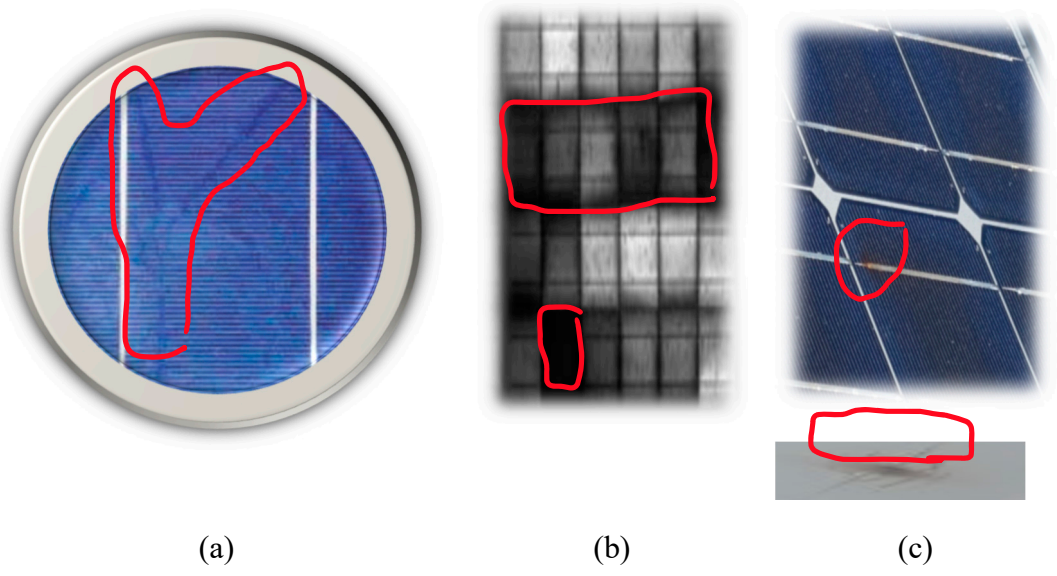

Figure 6. (a) PV module affected by snail track failure [122]. (b) PID failure detected by electroluminescence image [134]. (c) Hotspot burned the cell solder bonding and exhibited burn marks on the backsheet [135].

2.4. Backsheet

The backsheet is the last protection layer of the PV module that provides construction support to the PV module. It shields the modules' electrical parts from short circuit failure, ensuring perfect electrical insulation from various environmental stress factors such as water ingress from high relative humidity [136]. Failures and degradation in the backsheet can appear as cracks, discolouration, delamination, bubbles, and burn marks [127].

 doi:10.20944/preprints202311.0761.v1

The major cause of burn marks failure is hotspots, and this may lead the PV module to catch fire. For this purpose, a study conducted by Cancelliere and Liciotti [95] investigated fire reactions with four material arrangements on the basis of PET (Polyethylene Terephthalate) backsheet: 3-layers (PET/PET/Primer), 4-layers (PET/Aluminium/PET/Primer), 3-layers (Fluoro-Coating/PET/EVA) and PET layer with an outside and inside coating. The two backsheets, PET monolayer with an inside and outside coating, and the 4-layers (PET/Aluminium/PET/Primer) reacted slower to fire flame and had fewer damaged areas with no or less harm to EVA encapsulant. However, the monolayer with an inside and outside coating backsheet is favoured over the other as aluminium is electrically conductive and may result in less power production. PET backsheet was also nominated for a cracking comparison against backsheet made of PP (polypropylene) by Oreski *et al.*[137]. The comparison study employed a stress accelerated test to explore if PP backsheet has the same immunity as PET. They found that PP exhibited cracking after the same exposure time as PET which makes it a reliable substitution in PV backsheet industry. Even though, a suggestion by Elfaqih *et al.*[138] to mix the PP backsheet with 5% carbon fibre to provide greater strength and longer reliability against failure. They come up with their proposal after they investigated PP and PPCF (PP supported with carbon fibre) and found PPCF backsheet has higher tensile strength.

Investigations of the PV module's backsheet deployed in outdoor conditions was also conducted by Pascual *et al.*[139], where PV modules were deployed in an eight-MW plant, all of which were from the same manufacturer but with two backsheet types; PVF (fluorinated) and polyamide. The PV modules were deployed in 2011 and investigated after six years of operation. Visual inspection revealed that 14% of modules with polyamide backsheet suffered from cracks. Furthermore, polyamide backsheets were susceptible to chalking which is a decomposition of backsheet material into white powder that is considered a warning sign of abnormal degradation [140]. More than 90% of inspected PV modules of polyamide backsheet degraded by chalking while none of the PVF backsheets did. The strength of the PVF backsheet might be one of the reasons that drive researchers' attention e.g.[141,142] to search for effective ingredients to be utilized in stress-accelerated tests.

With regards to cracking, Mühleisen [143], developed a solution based on polyurethane paint to be coated at the early onset of the backsheet's cracks. The coating was examined for nearly two years in outdoor conditions and was also tested under stress accelerated test. Their results showed a significant reduction in crack progressing in the coated backsheet compared to the uncoated ones. The study of Mühleisen [143] is not the first of its kind, Beaucarne *et al*. [144] also fabricated a coated solution recognised as a flowable-silicone-sealant that can act in place to avoid early replacement of PV modules. They applied the solution on PV modules operated for less than 8 years with heavy backsheet cracks. These modules were of four types of backsheet; Co-extruded polyamide, PVF, PVDF and PET. The cracked backsheet modules were tested for insulation resistance and none of them passed the required standard level. After applying the coating, all of them restore a healthy level of insulation resistance even after applying stress accelerated tests for a thousand hours.

Preprints (www.preprints.org) | NOT PEER-REVIEWED | Posted: 13 November 2023 doi:10.20944/preprints202311.0761.v1

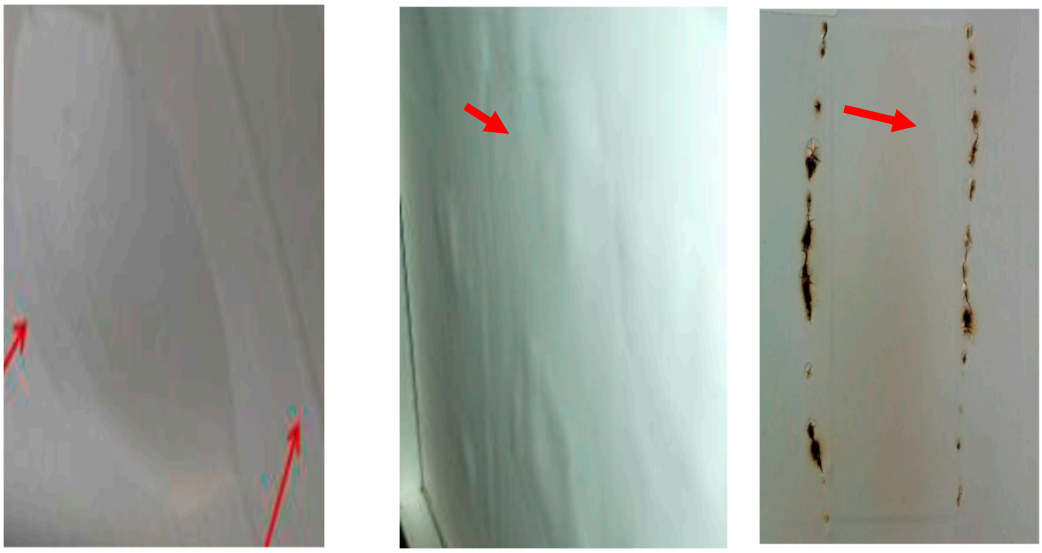

(A) (B) (C)

Figure 7. (A) Backsheet bubbles [127]. (B) Backsheet delamination [127]. (C) Burn marks were caused by a hotspot in the backsheet [135].

2.5. Junction Box and Bypass Diodes

A junction box (J-box) is attached to the PV module through adhesive material to regulate and provide a safe flow of the collected photocurrents in a PV module [145]. To guarantee the correct flow path of the current, bypass diodes are also installed inside the j-box in different configurations; overlap and non-overlap [146]. Failures in the j-box are mainly caused by low wiring quality, blown bypass diodes, corrosion and poor bonding to the PV module (delamination) caused primarily by high humidity [82]. Failure of the J-box may result in zero output of electricity, this was found by Bakir [147] in a recent assessment of a 23 MW PV plant mounted in Turkey. As of this, many studies e.g.[148,149] came up with novel techniques to monitor and protect J-boxes from failures. Most J-box failures allow water vapour to ingress, causing serious safety issues, initiating an electrical arc or causing hotspots [20]. Ong *et al*. [150] listed failures of J-box among the root causes of fire ignition in PV modules. Han *et al*. [14] investigated the condition of 177 mono-crystalline PV modules that operated for 22 years in a humid climate with an average temperature of 27.5°C. Most of the junction boxes of the modules had been seriously damaged and needed a replacement.

Furthermore, junction-box can degrade at a faster rate when exposed to high alteration of ambient temperature during the year. Daher *et al*.[151] evaluated the reliability of a 9-year PV system (270 modules) installed as off-grid that is expected to produce 62 kW in Ali Adde town, Djibouti. The PV system is exposed to the town's high temperatures with dramatic variation from winter to summer, where in the winter months its average temperature is 26.7 C and rises to a very hot temperature in the summer months with an average of 38 C. Out of 270 modules, 39% diagnosed with adhesive junction-box failure.

On the other hand, cold climates with high relative humidity like Grimstad, Norway led to the corrosion of junction boxes [38]. J-boxes and metal parts of PV modules operating in the so-called floatovoltaics structure, like PV systems deployed on the water in a floating construction, are too at higher risk of corrosion [152]. This urged Ghosh [153] to recommend that j-boxes should have a protection rating of IP67 when attached to PV modules mounted in a water-based environment. Unsurprisingly, dust was also found to corrode the PV module's junction box, Tabet *et al*.[154] inspect a module operating in a dusty environment for six years, exhibiting that j-box failed because of corrosion. This is in agreement with Lin and Zhan [155] that water-dissolvable salts represent more than 59% of dust composition in which ,whenever stuck to metal, react and cause corrosion primarily in humid environments.

Preprints (www.preprints.org) | NOT PEER-REVIEWED | Posted: 13 November 2023 doi:10.20944/preprints202311.0761.v1

Several PV failures were found to form hotspots making it necessary to protect the PV module. One means of protection is to use a bypass diode, although it has been criticised for being neither safe nor effective [68,156,157]. The existence of a bypass diode enables the current to flow over the defective solar cells, thereby protecting the PV module from thermal increases and hotspots. This is one of the main explanations why some PV manufacturers, such as AE-Solar, a German PV Manufacturer, attach a bypass diode to each PV cell [158]. One of the recurrent reasons for blown bypass diodes is the increase in their temperature due to long-term shading [159,160]. Also, it was indicated by Bansal *et al*. [82] that those bypass diodes that were exposed to over irradiance, in particular over 1400 Wm^{-2} are expected to be blown due to high-flowing currents.

Failure to detect poor bypass diodes may lead to serious safety issues [160,161]. Since bypass diodes are used to avoid PV failures that lead to hot-spotting, whenever they fail, the module loses its means of protection becomes vulnerable and, in the worst scenario, initiates fire [26,162]. Bakir [163] used an infrared imaging detection technique where he attached the thermal cameras to a drone to be flown over three solar plants that range between 2 and 3.5 MW. One of the plants has three PV modules with failed bypass diodes and as a result, their operating temperature increased by an average of 19.7 C. It was shown by Ghosh *et al.*[164] that the operating temperature of the PV cell undergoes shading failure decreased by nearly 50% when bypass diodes are functioning. Their experimental study aimed to explore if total cross-tied (TCT) array configurations is effective in preventing hotspot by allowing the bypass diodes to respond promptly in case of shading. And showed that bypass diode was only functioning if more than one cell was affected by shading and, therefore further investigations are required to pinpoint the optimal configuration of PV array that is able to activate bypass diodes even in the case of one shaded cell, like in the birds dropping situations.

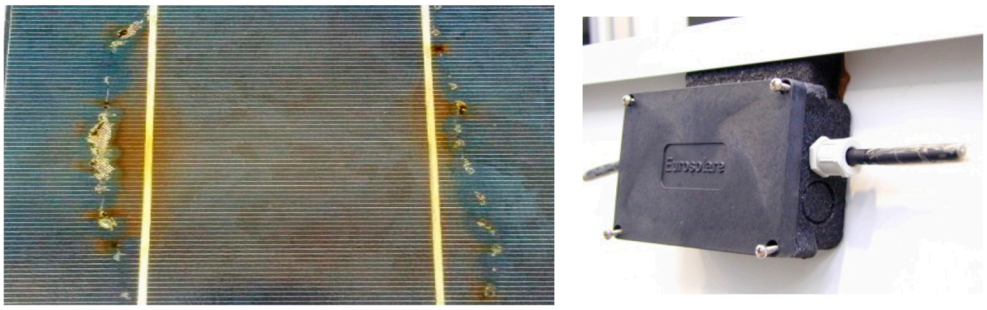

(a) (b)

Figure 8. (a) Failed bypass diodes led to hotspots [135]. (b) Poor bonding of j-box [134].

To conclude this section (2 to 2.5), PV failures can be classified based on their components. The same PV failure mechanism can be seen or experienced in more than one component due to the similarity of the materials, e.g. EVA presents in encapsulant and also in backsheet. Furthermore, EVA defect is usually considered the early sign of PV module degradation and failure as it is alongside PV glass representing the first defence line against weather stressors. Unlike snail track in PV cells, corrosion is another failure mechanism that can attack more than one component; solar cell solder, bypass and junction box, especially in humid environments.

The hotspot failure mechanism is considered the most severe failure that leads to catastrophic consequences. It deteriorates all PV module components if undetected, PV module affected by an elevated level of hotspot cannot be reversed and often requires a replacement. Thus, Identifying the initial stages of PV degradation can prevent potential hazards through proactive maintenance. Sometimes, it is even more effective to substitute a PV module that displays early onset of deterioration as it will guarantee all deployed modules in PV plants continue generating the healthier (expected) power, regardless of if their condition complies with the IEC 61215 standard [109]. Table 2 lists the reported PV failures from investigational studies within the last two years, classifying them on PV component basis.

Table 2. Reported PV failures from investigational studies within the last two years.

Component Impacted	Defect (Failure)	Type of PV (Poly-Si, Mono-Si)	Operational Time (Year)	Failure Detail	Country	Ref
Protective Glass	**Breakage**	Mono-Si	16 and 13	Two occurrences owing to poor transportation and vandalism.	Indonesia	[121]
		Poly-Si	20	None of the 43 PV modules affected by breakage glass.	Norway	[38] [39]
		Not Stated	Not Stated	52 modules affected in three PV plants ranging from 2 to 3 MW.	Turkey	[163]
		Poly-Si	6	Rare occurrences of glass breakage accompanied by cracked cells and dark EVA discolouration. Potential cause: hotspot, harsh weather (high wind speed and dust) and incorrect installation.	India	[31]
		Poly-Si	10	Less than 1% out of 2078 investigated modules. Possible causes: wind, hotspot and handling.	India	[32]
EVA	**Discolouration**	Poly-Si	5[(a)], 9[(b)], 5[(c)], and 10[(d)]	Dark[(a)], Light yellow[(b)], Dark[(c)] and Brown[(d)]	Ghana	[33]
		Mono-Si	15 [(a)] and 5[(b)]	Light yellow [(a)], and Light Brown[(b)]		
		Both Types	16 and 13	Not specified.	Indonesia	[121]
		Poly-Si	20	Nearly all investigated (43 PV modules) affected	Norway	[38] [39]
		Mono-Si	10	Two out of 156 PV modules displayed brown discolouration	U. S	[34]

doi:10.20944/preprints202311.0761.v1

		Both Types	11	Prevalent among all PV modules resulting in up to 18% reduction of *short-circuit current,* potentially brown discolouration[165].	Algeria	[35]
		Poly-Si	6	Rare occurrences of light discolouration in 10 MW PV plant.	India	[31]
		Mono-Si	11	Brown discolouration was detected in 10% of the PV modules.	Algeria	[36]
		Poly-Si	10	Roughly 14% of the 2078 investigated modules were affected by yellow and brown discolouration.	India	[32]
	Delamination	Both Types	8y-poly and 15y-mono	Rare occurrence with less than 4 impacted modules out of 104 of all types.	Ghana	[33]
			16 and 13	Several occurrences, especially in the 12-year PV system	Indonesia	[121]
		Poly-Si	10	Dominant among the 43 PV modules, mainly at the cell edge	Norway	[38] [39]
		Both Types	10	Rare occurrences, only 11 out of 2078 investigated modules, potential cause was weather condition.	India	[32]
		Mono-Si	10	All investigated (156) PV modules were influenced near the busbar, root cause expected to be the heat results from busbar's resistance.	U. S	[34]
		Both Types	11	Potential cause: the desert weather.	Algeria	[35]
		Mono-Si	11	25% of modules experienced delamination, some at the centres and others at the edges.	Algeria	[36]

doi:10.20944/preprints202311.0761.v1

Solar cells	**Cracks**	Mono-Si	5 and 15 years	Extremely rare only two were affected of 104 modules. Possible cause was unknown.	Ghana	[33]
		Poly-Si	20	Prevalent among the 43 PV modules, predominantly at the cell edge	Norway	[38] [39]
		Mono-Si	10	Few cracks were detected from PV modules inspected by EL imaging.	U. S	[34]
		Poly-Si	14	Results from EL imaging showed that 9 out of 10 modules have crack cells.	Germany	[37]
	Corrosion	Both Types	20	12 out of 104 modules were affected.	Ghana	[33]
	Snail Track	Both Types	5	Rare occurrence with less than 4 impacted modules out of 104 of both types. Claimed to be caused by manufacturing process.	Ghana	[33]
			16 and 13	Several occurrences, especially in the 12-year PV system.	Indonesia	[121]
		Mono-Si	11	Two out of 20 modules suffered from snail tracks, one of which was inked with cracked cells.	Algeria	[36]
		Mono-Si	10	30 out of 156 PV modules displayed snail track.	U. S	[34]
		Poly-Si	10	Roughly 1.5% of 2078 investigated modules were affected, with snail track often linked with cracked cells.	India	[32]
	PID	Poly-Si	20	One investigated by EL imaging, the cell's crack seems to be the cause of PID	Norway	[38] [39]
	Hotspot	Poly-Si	20	One investigated by IR imaging, suspected that derived from cracks.		
		Mono-Si	10	10 modules suffered from hotspots and displayed burn marks on the backsheet.	U. S	[34]
		Not Stated	Not Stated	One module was detected in a 2.7 MW PV plant.	Turkey	[163]

doi:10.20944/preprints202311.0761.v1

		Poly-Si	6	Suspicion in one module of one module. Potential cause: mismatch.	India	[31]
		Poly-Si	14	Three out of 10 modules showed hot spotting, detected by IR.	Germany	[37]
		Poly-Si	10	10 out of 2078 investigated modules were detected.	India	[32]
Back sheet	**Chalking**	Mono-Si	11	1 out of 20 modules.	Algeria	[36]
	Discolouration	Both Types	8	Nearly 14 modules were affected out of 104 of both types, specifically those lacking of mounting support.	Ghana	[33] [39]
		Poly-Si	10	11 out of 2078 investigated modules failed with burning and cracks. Possible cause is hotspots and failed J-boxes.	India	[32]
	Delamination	Mono-Si	10	29 out of 156 PV modules suffered from backsheet delamination failures like bubbles.	U. S	[34]
J-Box	**Corrosion**	Mono-Si	16	Several occurrences.	Indonesia	[121]
	Delamination	Both Types	13	Poor installation is potentially the cause.	Indonesia	[121]
		Mono-Si	11	1 module had a detached J-box.	Algeria	[36]
	Burning	Poly-Si	10	Only two out of the 2078 investigated modules were detected.	India	[32]
	Bypass diodes	Not Stated	Not stated	8 modules were detected in a 2.7 MW PV plant.	Turkey	[163]

Preprints (www.preprints.org) | NOT PEER-REVIEWED | Posted: 13 November 2023 doi:10.20944/preprints202311.0761.v1

3. Classification of Crystalline Photovoltaic Module Failures

Failures can be classified into different criteria based on the severity, location of the failure, and occurring time, whether occurs at the early installation or in the last years of warranty. Kuitche *et al.* [166] classify the failure types based on severity level, the severity of failure was mathematically estimated using Eq. (2.1) [166].

$$RPN=S \times O \times D \quad (2.1)$$

Where RPN is defined as the Risk Priority Number used as a rating guideline;

S: is the severity rating and it is rated from 1 to 10, where 1 refers to no apparent defect and 10 indicates no operation.

O: failure occurrence, and it is rated from 1 to 5, where 1 indicates failure is less likely to occur, and 5 indicates a frequent occurrence; at least once per month.

D: Detection of the failure and rated from 1 to 10. One indicates the failure will be easily detected, and ten is less likely to be spotted.

Similarly, Jordan *et al.* [44] adopted Eq. (2.1) to extract a classification method based on severity. They ranked the severity from 1 to 10, where 1 indicates there is no effect on the performance of the PV module and 10 points a severe impact on the performance accompanied by a safety hazard. Within their classification, hotspot failure ranked 10, and a minor delamination failure rated 1. Tsanakas *et al.* [51] classified PV failure differently based on optical and electrical shortages. Failures that can be visually identified were categorised as optical failures and those that require measurements of their parameters were categorised as electrical failures. On the other hand, Kontges *et al.* [20] classified PV failures into three categories based on the expected time of occurrence in PV lifecycle: infant-life, mid-life, and wear-out failures. Infant-life failures are the ones that appeared in the early life of PV operation. Mid-life failures arise after eight years of operation, whereas wear-out failures are failures that emerge just before the end of the module's lifetime. A recent review by Hong and Pula [167] classified PV failures based on connections; whether the failure represents a ground or line-to-line fault. A list of PV failure classification is summarised in Table 3.

Table 3. Photovoltaic failures list classified by three different reviews.

Photovoltaic Failure	**Classified by Jordan *et al.* [44] Classification Categories: Severity 1 to 10.**	**Classified by Tsanakas *et al.* [51] Classification Categories:** *a) Optical* *b) Electrical* *c) Not Classified*	**Classified by Köntges *et al.*[20] Classification Categories: a) Infant-Life b) Midlife- c) Wear Out**	**Classified by Hong and Pula [167] Classification Categories: a) Mismatch b) Ground c) Line D) Arc (E) Other**
Hotspot	10	Electrical	Not Classified	Other
Encapsulant Delamination	Minor Delamination: 1	Optical	Mid-Life	Mismatch

 doi:10.20944/preprints202311.0761.v1

	Major Delamination: 5			
Encapsulant Discolouration	3	Optical	Mid-Life	Mismatch
Solder Bonding	8	Electrical	Wear Out	Ground and Arc
Glass Breakage	5	Optical	Early Life	Other
Cracked Cell	5	Electrical	Mid-Life	Other
Bypass-Diode	5	Non-Classified	Mid-Life	Other
Junction-Box	5	Electrical	Infant-Life	Arc

4. Effect of Environmental Stress Factors on PV Degradation

Each manufactured component in the industry has a tolerance rating in relation to environmental stress factors which include temperature, humidity, wind, ultraviolet snow and dust. The PV module component has no exception in this equation[168]. Harsh weather including but not limited to high and low temperatures, high relative humidity, dust storms, snowstorms, and high UV index, are aspects of environmental stress factors that reduce the PV module's efficacy and trigger degradation in its early lifespan. For instance, increases in ambient temperature above 25 ^{0}C reduces the power production of PV module [169,170].

Failures such are potential induced degradation, encapsulant discolouration, and delamination were listed to be triggered by high ambient temperature by Köntges *et al* [20]. Humidity triggers the adhesion of the module's back sheet and raises safety concerns in the PV system when water vapours penetrate the module's conductor parts and junction boxes [14,20]. Humidity has a significant contribution to the corrosion of the j-box as it first deteriorates the bond force of cohesive material and secondly allows water to breach and react with metal [171]. Dust particles and snowing were reported to cause shading failures and reduce power output significantly [3]. Both extreme cold and hot climates were found to increase the degradation rate of PV modules as well as increase the expansion of cracked cells [32,134,172].

Santhakumari and Sagar [171] reviewed the literature focusing on failures related to weather condition and their contribution to the degradation of the photovoltaic system components, including batteries, cables, and inverters. Their review concluded that high ambient temperature, relative humidity, dust, sandstorms, and hailstorms highly trigger PV failures, causing optical and electrical losses. These environmental stress factors are found to trigger encapsulant degradation, corrosion, and glass breakage. The review [171] also addressed some of the experiments that have been conducted to tackle harsh environmental stress factors. For instance, sprinkling water on the PV panels was an efficient technique to reduce the thermal operating temperature of the PV module. The kinds of failure classified by Santhakumari and Sagar [171] to be triggered by high relative humidity were also found by Chandel *et al*. [62] in deployed mono-crystalline PV modules in a humid environment in India, with a nearly doubled degradation rate of 1.4%.

Dust accumulation is another environmental stress factor that decreases the power output by causing shading on the PV surface, it occurs in locations where dust storm is common like the Middle East and Africa. The dust particles are either scattering in the atmosphere or accumulating on the PV module surface [173]. When dust scatters in the atmosphere, it minimises the irradiation reaching the earth's surface and converts it to diffuse irradiance, slightly reducing the overall power. In contrast, dust accumulation on the PV surface directly impacts the power output and thus brings more attention to be investigated more extensively. It motivates researchers who live in harsh weather

Preprints (www.preprints.org) | NOT PEER-REVIEWED | Posted: 13 November 2023 doi:10.20944/preprints202311.0761.v1

environments to conduct more studies during dust storms [174], while others have set up lab experiments to investigate different dust particle properties on PV modules [175,176].

Saidan *et al.* [174] compared the electrical parameters between PV modules at different periods of dust accumulation. They concluded that the reduction of short-circuit current and the power output became greater for longer periods of dust accumulation. That is, I_{SC} was decreased by fourfold when dust accumulated for one month compared to one day. This is in agreement with Said and Walwil [177] who investigated dust accumulation on deployed PV modules in Dharan, Saudi Arabia; the I_{SC} reduced greater in a more extended time of dust accumulation.

Many factors need to be considered to address PV dust and snow accumulation; tilt angle is one of them. Sayigh *et al.* [178] experimented with PV modules operated in the field for 38 days at different tilt angles ranging between 0^{o} to 60^{o}. They found that dust accumulation increased dramatically when the tilt angle decreased, causing a reduction in the PV transmittance. This was also experimented and confirmed by Said and Walwil [177]. Both Elminir *et al.* [179], and Said and Walwil [177] showed that the dust accumulation increased fivefold at a tilt angle of 0^{o} compared to a tilt angle of 90^{o}. Properties of dust particles, weather conditions, and dust adhesion force also play a vital role in tackling the dust accumulation problem. For example, the adhesion force for the larger dust particles was higher than the smaller ones [176,177].

A lab experiment conducted by Mehmood *et al.* [175] identified the material components of the dust particles found in Dhahran, Saudi Arabia and their mud character when they react with humidity on two PV surfaces: glass and polycarbonate. The dust particles collected from the PV module's surface were mixed with different concentrations of deionized water, applied to the glass and polycarbonate and then dried for two days. Their results showed that the glass's transmittance was reduced by 9% more when compared to the polycarbonate.

It is essential to assess the weather conditions for targeted geographical locations when installing a PV system, studying the risks and economic feasibility of extra application of immune material against existing weather stressors. Some weather stressors require advanced materials to be overcome like high UV index and humidity, while others may only require continuous monitoring such as regular cleaning of dust and snow. Hence, early planning and assessment ensure a reliable operation of the PV system, as well as reduce the risk of lost revenue for PV operators by ensuring maximal power generation. For instance, keeping PV surface unclean in a dusty environment was reported to cause a decrease in power generation by 18% in just one month of dust accumulation [174]. Table 4 lists some recent studies that highlighted weather conditions' effect on PV.

Table 2 PV studies that highlighted weather conditions within the last two years.

Weather Condition	Weather Highlight	Failure Modes Detected or Explored	Type of PV (Poly-Si, Mono-Si)	Life-Time (Year)	Country	Ref
Subtropical climate with moderate humidity level	Hot	Glass breakage- EVA discolouration -Soiling-Cracked cell-Hotspot.	Poly-Si	6	India	[31]

Preprints (www.preprints.org) | NOT PEER-REVIEWED | Posted: 13 November 2023 doi:10.20944/preprints202311.0761.v1

and high temperature.						
Semi-desert climate, considerably hot and dry weather.	Hot	Glass breakage- EVA discolouration -Soiling- EVA delamination- Cracked cell- Snail track- Metal Corrosion- Backsheet cracks and burns.	Poly-Si	10	India	[32]
Dry equatorial climate. The average temperature is 28 °c and 30 °c and the average humidity is between 60% and 75%.	Dry and hot	EVA discolouration – Metal Corrosion- Backsheet defects.	Mono-Si	Between 0 to 5	Ghana	[33]
Wet semi-equatorial climate. The average temperature ranges between 26 °c and 30 °c and the average humidity is between 70% and 80%.	Hot and humid	EVA discolouration - EVA delamination- Metal Corrosion- Backsheet defects.	Poly-Si	Between 6 and 10.		

 doi:10.20944/preprints202311.0761.v1

Desert climate hot and dry with moderate to high relative humidity, throughout the year.	Dust	Experimental study to address dust effect. Soiling reduced power production by 9% within 30 days.	Mono-Si	Not-stated	Oman	[180]
Dry, hot in the summer and moderate temperature with frequent rainfall in the winter	Dust	PV modules were kept for 6 months for soiling evaluation, result showed 20% power loss despite rainy days in 2 months.	Mono-Si	Not-stated	Iran	[181]
Dry, hot in the summer and moderate temperature in the winter	Dust	PV modules were kept for 6 months for soiling evaluation, an average of 18% of power loss was recorded.	Mono-Si	Not-stated	Iraq	[182]
Cold, frequently accompanied by snowstorm	Cold Snowing	Analysis model to forecast PV production expected 80% power loss if the snow thickness is 60 mm.	Not-stated	Not-stated	China	[183]
One city has dry and hot weather whereas the other has less temperature weather.	Hot	Comparison between two PV systems installed in two cities. The one installed in the Mediterranean climate is superior, despite the high humidity level.	Both	Not-stated	Morocco	[184]

 doi:10.20944/preprints202311.0761.v1

Hot accompanied by high relative humidity; up to 85 %	Hot and Humid	EVA discolouration and delamination- Snail track- Metal Corrosion- Backsheet cracks and burns-Hotspot	Mono-Si	10	U. S	[34]
Dry and hot climate, with frequent sandstorms located in the desert.	Dry and hot	EVA discolouration and delamination- Metal corrosion.	Both Types	11	Algeria	[35]
Hot with a high relative humidity range; average is 67%.	Hot and humid	EVA discolouration and delamination- Snail track- Metal Corrosion- Soiling-Backsheet chalking- J-box delamination	Mono-Si	11	Algeria	[36]
Moderate climate with considerable high relative humidity can reach 83% in the winter months.	Humid	EVA discolouration and delamination- Cracked cell- Metal and bypass corrosion-hotspot-PID.	Poly-Si	14	Germany	[37]
Cold and humid, average temperature range between - 6.7 °c and 21°c, average humidity range	Cold	Glass breakage- EVA discolouration and delamination- Cracked cell- Metal Corrosion- hotspot.	Poly-Si	10	Norway	[38] [39]

between 30% and 99%.						

5. Detection of PV Failures

Depending on the connection types of the PV system, whether it is grid-connected or standalone, failures occurred on two different sides DC and AC. They often occur on the DC side when the system is standalone, whereas they similarly exist on the AC side when connected to the grid. Distinguishing them can be achieved by monitoring the system's power output; it reduces and rarely leads to a blackout in DC failure but causes a total blackout when a failure occurs on the AC side [185].

Madeti and Singh [185] reviewed the literature and classified all failure detection techniques into two groups;(a) fault detection based on the ground that involves monitoring sensors and (b) fault detection based on a space monitoring system. The latter group is cost-effective owing to the lack of instrumental sensors but depending on weather conditions its accuracy can be reduced dramatically. The sensors employed in ground-based techniques are set to observe the major electrical parameters such are current, voltage, and power. These parameters vary based on the PV system's connection type; for instance, grid impedance exists in a grid-connected system, but not in a standalone system [185].

Each type of PV failure requires a different tactic to be detected. For example, detection tactics employed in optical failures are different from those employed in electrical failures. Optical failures may be seen by the naked eye, whereas electrical losses require instruments to monitor, store data, and perform analysis. Furthermore, detection techniques for failures on the AC side, e.g., PV converter, and power blackout of the grid, are utterly different from those on the DC side [185]. This review will briefly review the failure detection techniques proposed on the DC side (PV module components).

According to Pillai and Rajasekar [186], for the detection technique to be effective, it should meet the following criteria: (1) Able to detect failures without interfering with power or causing blackout (2), Able to pinpoint the failure, (3) Cost-effective and flexible (4), Simple and not complicated in structure and (5), Can be applied to different variety of PV systems. Madeti and Singh [185] classified failure detection techniques of the DC side into six categories; electrical characterization, infrared imaging, visual inspection, ultrasonic inspection, electroluminescent imaging, and lock-in thermography. Nearly the same classification was presented by Santhakumari and Sagar [171], but with fewer details or different naming, e.g. electrical characterization was referred to as indoor testing using the solar simulator. Twelve detection techniques were under electrical characterization listed in the Madeti and Singh [185], five of them reviewed in more detail by Mellit *et al.* [187]. Those five techniques were signal and processing, *I-V* characteristic analysis, power loss analysis, voltage and current monitoring, and machine learning detection techniques.

5.1. Visual Inspection

The first step to detect PV failure is to view the PV modules from different angles. Visualizing techniques have been demonstrated and reviewed by the international standard IEC 61215 [188]. The standard considered broken, cracked, and misaligned module surfaces as well as bubbles of the encapsulant as significant defects. Failures such are delamination, mild discolouring, corrosion, j-boxes, and shading could be visualised by the naked eye without employing other detection techniques [82,187]. Moreover, some researchers proposed the use of drones with installed cameras to visualize PV plants more effectively, e.g., [147,189].

5.2. Infrared Imaging

Infrared imaging is a detection technique based on the solar cell's reversed biased circulating current in a PV module [190]. In case of failure, the solar cell dissipates heat which an infrared camera can detect. Hotspots, as well as microcrack failures, sometimes cannot be seen by the natural human

Preprints (www.preprints.org) | NOT PEER-REVIEWED | Posted: 13 November 2023 doi:10.20944/preprints202311.0761.v1

eye. Still, they are caught by infrared imaging. Predicting failure before taking place is a major advantage of this technique. On the other hand, drawbacks will be staffing and expensive costs [186]. The working principle is usually started by storing images of a healthy PV module to compare them to a faulty module when needed. This technique can detect hotspots, breakage of solar cells, disconnection, and PID failures [82].

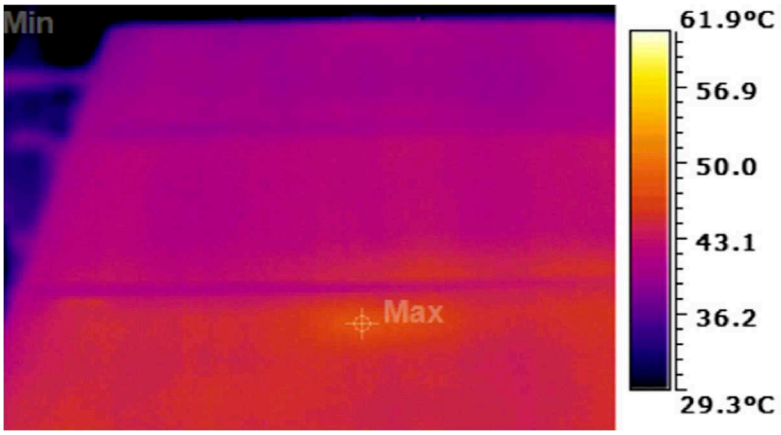

Figure 9. Infrared imaging to discover high-temperature cells in a PV module [186].

5.3. Electroluminescence Imaging

This technique is used to detect a potential cracked cell by pinpointing the low contact area of a PV module [191]. The working principle of this technique is to look into the recombination losses (shunt defects) created by an injected current to the solar cell metallic contact [192–194]. In addition to detecting cracked cells, snail tracks, and PID failures can be seen using EL imaging [82]. The lock-in thermography detection technique has nearly the same working principle as EL but was found superior and more sensitive in detecting failures [122].

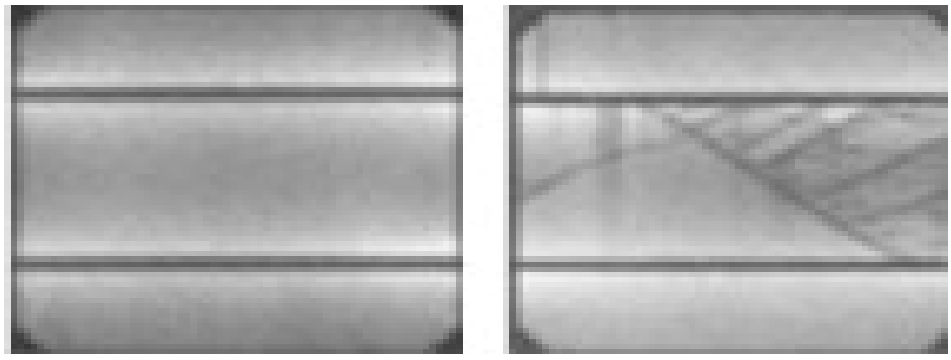

Figure 10. (a) EL imaging of a healthy monocrystalline solar cell. (b) El imaging of a cracked monocrystalline solar cell [195].

5.4. Ultrasonic Inspection

The detection technique of ultrasonic inspection compares the frequency signals of a healthy and a faulty cell obtained by an ultrasonic transducer [196–198]. The resonance frequency intends to decrease when detecting a defective cell [197,199]. The ultrasonic technique is mainly used to detect cracked cells in a PV module. An advantage of the method is that it infers the severity level of the cell crack based on the range of the frequency's bandwidth [197].

Preprints (www.preprints.org) | NOT PEER-REVIEWED | Posted: 13 November 2023 doi:10.20944/preprints202311.0761.v1

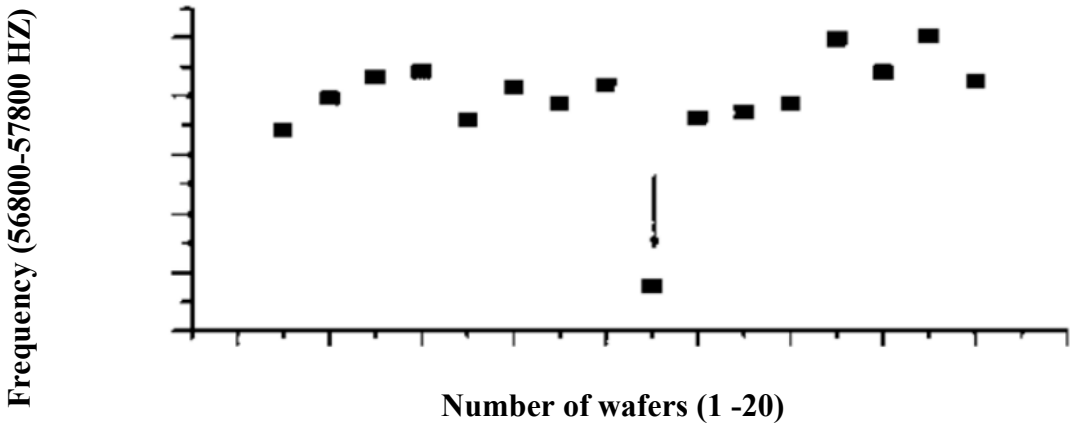

Figure 11. Ultrasonic inspection for several cell wafers showing cell No.11 has an abnormal reduction in frequency, indicating a crack failure [196].

5.5. Electrical Characterization

Electrical characterization has been claimed to be the most common detection technique for PV failures [200]. This detection technique focused on monitoring and spotting any changes in the PV system's electrical parameters. It was reviewed by Mellit *et al.* [187] and referred to as a signal-processing approach that involves protection devices such as over-current protection devices. Pillai and Rajasekar critically reviewed protection devices [186], explaining the limitations and drawbacks of detecting a failure instantly, particularly under low irradiance, which may lead to serious safety issues and catastrophic failure. For instance, delayed response from over-current protection devices when PV fails leads to an electric arc or fire [187].

I-V curve, power losses, and PV module's temperature, all of which can be used to detect PV failures. For instance, if the temperature of the PV module increases at hotspot failure, sensors can be put in place to detect abnormal increases [201], and further, Insulation monitoring devices evaluate the resistance between the current-carrying conductor and the ground to detect ground failure [202]. Fuses are able to calculate the residual system's current [203].

One technique of using residuals to detect failures is typically the simulation of a healthy PV module to obtain the maximum voltage (V_m), maximum current (I_m), and power values and then compare them with the received actual data. Residuals (the difference between the simulation and the experimental values) indicate the existence of PV failure. Depending on the residual extent, the type of failure can be predicted [204,205]. Harrou *et al.* [205] used this method as an indicator of abnormal changes in the PV system. However, they concluded the monitored parameters were insufficient to detect extreme degradation and partial shading failures. Elyes *et al.* [204] used the residual technique and reached the same result as Harrou *et al.* [205], predominantly for shading failures, thus, it will be more effective to include other *I-V* parameters as an indicator such as short-circuit current and fill factor.

One obstacle preventing accurate detection of PV failures was obtaining noisy data from measurements. Harrou *et al.* [205] focused on detecting four types of PV failures on the DC side; open circuit, short circuit, partial shading, and degradation failures. In order to detect those failures accurately, they had to use a wavelet-based multiscale tool to separate the noisy measurement data. Elyes *et al.* [204], also concluded that using wavelet-based multiscale, anti-noise techniques, increased the accuracy in the detection of PV failures. Noisy data seems to be an obstacle in Ali *et al.* [206] ending up suggesting to separate them using noise separation devices or working out efficient ways for noise separation. However, with advanced technologies at present, artificial intelligence (machine and deep learning) in particular, noisy data has been tackled in many recent studies, e.g. [207,208], that is; the accuracy of PV failure detection was robust even with the presence of noisy data and only neglected effect was observed.

Preprints (www.preprints.org) | NOT PEER-REVIEWED | Posted: 13 November 2023 doi:10.20944/preprints202311.0761.v1

5.5.1. Detection Techniques Using I-V Curve Parameters

The *I-V* curve shows the output combinations between voltages and currents, delivering the values of major parameters; short-circuit current, open-circuit voltage, maximum power output, and fill factor. Modelling of healthy or expected *I-V* curves and power output via engineering modelling programs are also classified under electrical characterization and was referred to as "model-based difference measurements" by Pillai and Rajasekar [186]. One of the reasons for the *I-V* curve to be simulated, instead of obtaining them experimentally, is the risk associated with performing faulty operation scenarios in a real PV plant which may get out of control [209].

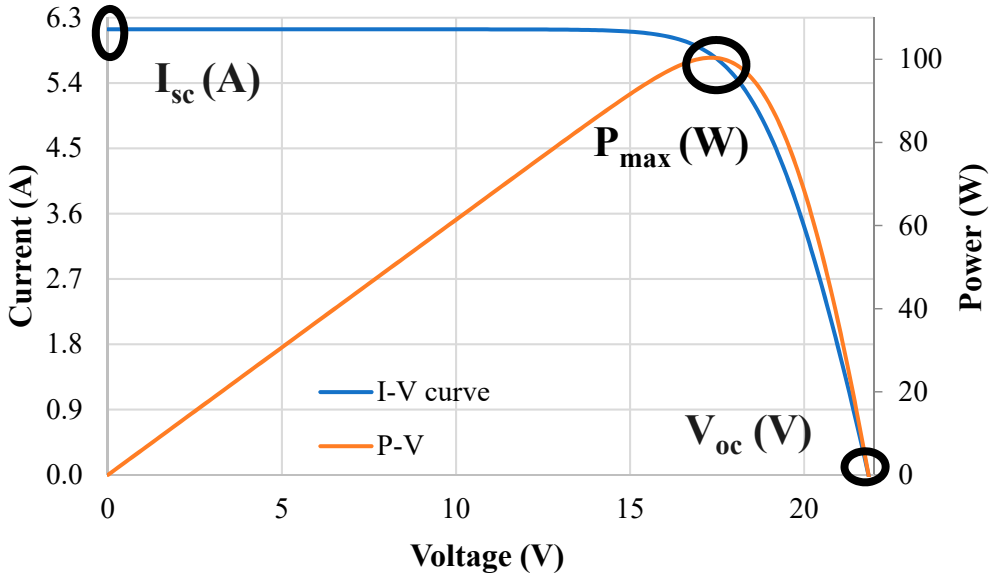

Figure 12. Current-voltage and Power-Voltage curves display the major parameters of a solar cell; I_{sc}, the current at zero volts, V_{OC}, the voltage at zero amps, and P_{max}, the maximum power output.

Chen *et al.* [210] investigated four failure modes and recorded their impacts on the *I-V* curve. Short circuit failure was found to decrease both P_{max} and V_{OC}. Degradation failure can be observed when a reduction in the *I-V* slope accompanies a gradual decrease in P_{max}. I_{SC} was decreased in open-circuit failure. In case of partial shading failures, the *I-V* curve will be distorted, forming multiple P_{max} points; one before shading and one after shading. Ali *et al.* [206] fabricated three shading scenarios on a PV string that contains three polycrystalline modules; firstly, one-third of two modules were shaded, secondly, three cells in each module were shaded and lastly, half cells in each module were shaded. As a result, *I-V* curves were distorted, and V_{OC} decreased in all three scenarios, at most in the third scenario with a 68% reduction.

Köntges *et al.* [20] agreed with Ali *et al.* [206] that shading failure distorts the *I-V* curve, creating multiple P_{max} points. They also listed the effect of various PV failures on the *I-V* curve; I_{SC} is affected mainly by optical failures and losses of transparency, EVA discolouration, glass breakage and shattering, and EVA delamination. It is also affected by disconnected soldering of the cells, PID, and cracked cells in the PV module. Whereas V_{OC} is affected by defective bypass diode, PID, and disconnected soldering of the cells. The fill factor is affected by delamination, corrosion, and cracked cells. All PV failures were found to reduce P_{max} except for the bypass defect.

The awareness of the electrical characterization's boundaries assists in training supervised machine learning algorithms by looking for deviations from their previous relationships to detect PV failure and degradation. Chine *et al.* [211] implemented artificial neural networks (ANN) to detect eight types of faults: shading caused by snow and soiling. A probabilistic neural network (PNN) algorithm was implemented to predict and classify three failure mechanisms by Garoudja *et al.* [209] and was found superior and more efficient than ANN even in the presence of noise. The substantial surge of published studies that proposed or developed artificial intelligent models to detect PV

 doi:10.20944/preprints202311.0761.v1

failures demands a review to arrange, compare and classify them. Researchers in recent years were aware of this gap and many reviews were conducted as a result e.g.[167,212–216].

5.5.2. Detection Degradations and Failures Using Shunt and Series Resistances

Modelling of the *I-V* curve's major parameters via mathematical equations, e.g. short circuit current and open circuit voltage, assists in extracting the values of other key parameters [217,218], namely series resistance and shunt resistance. As most PV failure and degradation modes will severely impact these parameters, quantifying them will significantly enhance detection models of PV defective modes [219]. Nonetheless, precise extraction of series and shunt resistance values is challenging [217,218] and thus many researchers have developed approaches to optimise an extraction technique to estimate their range values, e.g., [220–224]. While accurate parameter extraction might be challenging, estimating their values' range is still vital for the healthy operation of PV modules.

The shunt resistance offers a pathway for the photogenerated current, allowing it to bypass the PV equivalent circuit whereas the series resistance infers the solar cell components' resistances altogether such as the cell's base and busbar resistances. The series resistance increases in the presence of PV failures or degradation. It has been claimed that degradation mechanisms influencing series resistance are the most prevalent degradation mechanism after EVA discolouration [225]. Besides, it has greater severity; Wohlgemuth and Kurtz [40] stated increment of series resistance in PV modules may lead to disastrous consequences resulting from fire. In contrast, a higher value of shunt resistance indicates a safe operation of the PV cell as it directs most of the generated photocurrents to flow through one healthy path [67,226]. Conversely, when it is lost through alternative paths, the R_{sh} reduces significantly which ultimately leads to a severe drop in overall power production [67,226,227].

Kaplani and Kaplanis [228] investigated PV panels that were deployed for twenty years. They discovered that an 80% reduction in the R_{sh} and a 50% increment in the R_s were strongly linked to the PV panel's degradation, leading to 11% power loss. Furthermore, power degradation occurred as a result of several failures that directly impacted and reduce the shunt resistance including soldering defects, microcracks, shading, and hotspots [229,230]. Most of these failures were found to directly impact and increase series resistance too [225,231,232]. It can be noted that the majority of PV defects summarised by Tsanakas *et al.* [51], particularly the electrical ones, have been found in the literature to decrease R_{sh} and increase R_S. Based on this as well as other findings e.g. [83,219], the shunt as well as series resistances appear as strong predictors of PV failures and deterioration. Optical failures such as EVA delamination were found to lower shunt resistance and increase series resistances. Gxasheka *et al.* [233] compared the parameters of five deployed PV modules. The one affected by delamination had approximately 50% lower shunt resistance accompanied by a 61% increment in series resistance.

The effect of encapsulant discolouration, the most prevalent EVA defect, was also determined by Rajput *et al.* [234] to decrease shunt resistance. However, a study by Sinha *et al.* [235] compared two module pairs that operated for 20 years in India, one in each pair had brown EVA discolouration. They assumed there was no evident link found between brown EVA discolouration and shunt resistance decrement. This is perhaps due to the PV module receiving less illumination when EVA is discoloured [236] and as stated by Ruschel *et al.* [237] the shunt resistance increases when solar illumination decreases. However, this can be applied if the EVA experiences the same discolouration level across the PV module. Otherwise, different levels of EVA discolouration might have the same effect as minor shading and will lead eventually to decreased shunt resistance.

On the other hand, electrical failures, which are unlikely to be spotted by the naked eye [51], such as microcrack failures, were found by Zhang *et al.* [238] to decrease R_{sh} significantly. In their study, low shunt resistance was spotted from the short-circuit current slope in the *I-V* curve of a module with cracked cells whereas the increment in series resistance was minor unless the range of irradiance was between 250-475 Wm^{-2} [238]. Saavedra *et al.* [130] also experimentally investigated PV modules with cracked cells and reached the same conclusion as Zhang *et al.* [238], but experienced a

 doi:10.20944/preprints202311.0761.v1

greater increment in R_S. Potential-induced degradation was also directly linked with shunt resistance reduction and series resistance increment [239–241]. Myer and Dyk [66] simulated a PV module that consisted of 36 cells with 30% of the cells under shading failure to analyse the effect of shading on electrical parameters. In their findings, both shading and hotspots, when presented, significantly lowered the shunt resistance.

Degradation and many PV failures were associated with low shunt resistance and increased series resistance, making it vital to explore their behaviours when the solar cell degrades. A MATLAB study conducted by Dhass *et al.* [242] displayed that a reduction in shunt resistance caused a significant decrease in short-circuit current compared with open-circuit voltage. Another software program was employed by Dyk and Meyer [243] for the shunt resistance reduction effect, they found that a decrement in shunt resistance reduced P_{MAX}, V_{OC}, and fill factor with a slight increase in I_{SC}. Conversely, Sarkar [244] simulated the reduction of the R_{sh} effect using SPICE and showed that the reduction of shunt resistance leads to a greater decrement in open-circuit voltage instead of short-circuit current. It can be noted that the outcome discrepancies were due to the studies [242–244] relying on simulation software programs.

Several practical experiments have also been conducted and published in the literature; back in 1969 Kennerud [245] investigated a cadmium sulphide (CdS) solar cell, applying the Newton-Raphson technique to solve the *I-V* equations. Then, he manipulated the electrical parameters, including the R_{sh} *and the* R_s, to examine their influence on the *I-V* characteristics. The findings were experimentally verified and demonstrated that a decrease in shunt resistance was associated with a reduction in open-circuit voltage while increasing in series resistance was linked to a reduction in fill factor. Rummel *et al.* [246] fabricated a twelve-cell mono-crystalline module to explore the effect of 24 scenarios of shunt resistance levels at different irradiance levels, falling from 1000 W m^{-2} down to 90 W m^{-2}. A significant drop in the module's efficiency was observed after reducing the shun resistance, particularly with the lowest shunt resistance level. With the assistance of electroluminescence (EL) imaging techniques, Roy and Gupta [227] investigated images of solar cells exhibiting low shunt resistance levels linked with faulty operations such as hot spots. The shunt resistance was reduced artificially to six levels from 0.3 kΩ to 0.001 kΩ. The results showed darker images for the cell with reduced R_{sh}, with the level of darkness becoming more intense with the lowest levels of shunt resistance.

To sum up, it can be noticed from the literature that numerous studies were conducted to explore the shunt and series resistance effect as they are directly linked to most PV failures. Despite that, not as many studies employ them as indicators or predictors, predominantly studies related to series resistance, in the detection of PV failures or degradation. Al Mahdi [247] fulfilled the gap of shunt resistance in terms of PV degradation by developing a lab experiment that gradually and artificially decrease the shunt resistance of poly-crystalline solar cells to propose a detection model. It was found that critical degradation of PV cells occurred when shunt resistance decreased to 100 Ω.cm^2. Further experimental investigations for employing shunt and series resistances are needed to arrive at comprehensive and robust detection techniques for PV failures. Table 5 lists the most recent review studies about some detection techniques of PV failure mechanisms.

Table 5. Most recent review studies of some detection techniques.

Detection Technique	Highlight	Ref
Infrared Imaging (IR)	How PV benefits from IR and what can be done to expand the IR application in PV with the assistance of machine learning models.	[190]

 doi:10.20944/preprints202311.0761.v1

Electroluminescence (EL) and Deep Learning	A brief review of EL imaging in detecting micro-cracks failure modes with useful comparison to IR technique and the feasibility of using them in artificial intelligence models.	[248]
Machine Learning	Review of ML studies, underlining their accuracy in detecting PV failure modes. Highlighting the common models namely, Super Vector (SVM) and Neural Network (ANN).	[249]
Deep learning	Comparing Deep Learning models, their pros and cons as well as proposing a future path for enhancement.	[250]
Electrical Characterization	Reviewing and comparing detection techniques in grid-connected PV plants.	[251]

6. Conclusion

This review has entailed a body of knowledge by highlighting the global growth in PV modules deployment, stressing the need for understanding the reported PV failure behaviours and how they are initiated. When they occur, they lead to higher degradation rates causing a significant reduction in power output and, in the worst-case scenario, may become catastrophic. Most literature reviews of PV failures are based on the severity and frequency of occurrence of failures. This review takes a different perspective and focuses on failure mechanisms based on PV module components, reviewing each component's susceptibility to failures.

Looking into the literature in depth allows for extracting the root cause of some failure and degradation mechanisms. For instance, UV, one of the environmental stress factors, is considered the root cause of the most common degradation, i.e., encapsulant EVA discolouration that is responsible for the emergence of most optical failures, such as corrosion and delamination. Shading, glass breakage and soldering defects, on the other hand, can cause hotspot failure. Most PV degradation mechanisms lead to disastrous consequences, including human fatalities, when undetected or neglected.

In terms of failure detection techniques, it was pointed out that they should be simple, applicable in most PV systems, cost-effective, accurate, and detect failures at low solar irradiance. Typically, detection starts with visual inspection and then employs more instrumental devices like infrared imaging. However, these devices are costly, require more labour work, and are time-consuming and uncomprehensive, i.e., designed only to detect limited types of failures. In contrast, electrical characterization, which includes monitoring the power or the *I-V* curve, infers most PV failures from the shifts in the produced parameters. That seems to explain why it is the most common detection technique. Electrical characterization detection techniques were detailed in several reviews, but they have a gap for engaging shunt and series resistances. This review details their effect, evaluating the possibilities for utilizing them in electrical characterization. Which in turn, paved the road for future studies to investigate *I-V* measurements under changes in shunt and series resistances. Thereby allowing models to be developed in a simple, applicable, comprehensive, and novel way to facilitate early intervention to avoid catastrophic deterioration and ensure continued safe and productive operation of the PV systems.

Acknowledgments: Hussain Al Mahdi would like to acknowledge PhD funding support from the Saudi Ministry of Education.

List of Abbreviations

AM1.5G	Standard Solar Spectrum
EVA	Ethylene Vinyl Acetate
FF	Fill Factor of the solar cell
G	Solar Irradiance
I_{01}	First Saturation Current of the solar cell
I_{02}	Second Saturation Current of the solar cell
I_m	Maximum Current Output at the solar cell's current-voltage curve
I_{SC}	Short-circuit current of the solar cell
IR	Infrared Imaging
$I-V$	Current-Voltage Curve of the solar cell
J-box	Junction Box, a component of photovoltaic module
PDMS	Polydimethylsiloxane, a type of polymer used as an encapsulant in photovoltaic modules
PET	Polyethylene terephthalate, a plastic material used as a backsheet in a photovoltaic module.
PID	Potential Induced Degradation
P_{max}	Maximum Power Output, the maximal power produced by the solar cell
PV	Photovoltaic
RPN	Risk Priority Number used for rating guideline
R_{sh}	Shunt or Parallel Resistance of the photovoltaic solar cell
R_s	Series Resistance of the solar cell
SPICE	Simulation Program with Integrated Circuit Emphasis
STC	Standard Test Condition
TPU	Thermoplastic Polyurethane
UV	Ultra-Violet
V_{OC}	Open-circuit voltage of the solar cell
V_m	Maximum Voltage Output at the solar cell's current-voltage curve

Reference

1. Li, L.; Lin, J.; Wu, N.; Xie, S.; Meng, C.; Zheng, Y.; Wang, X.; Zhao, Y. Review and outlook on the international renewable energy development. *Energy and Built Environment* **2020**.
2. Green, M.A. How did solar cells get so cheap? *Joule* **2019**, *3*, 631-633.
3. PSE, A. Fraunhofer Institute For Solar Energy Systems ISE. *Photovoltaics Report.(2022)*.
4. IEA. *Net renewable capacity additions by technology, 2020-2022*; IEA.: Paris May/2021.
5. Goetzberger, A.; Hebling, C.; Schock, H.-W. Photovoltaic materials, history, status and outlook. *Materials Science and Engineering: R: Reports* **2003**, *40*, 1-46.
6. Green, M.A.; Dunlop, E.D.; Hohl-Ebinger, J.; Yoshita, M.; Kopidakis, N.; Ho-Baillie, A.W. Solar cell efficiency tables (version 55). *Progress in Photovoltaics: Research and Applications* **2019**, *28*.
7. Peike, C.; Hädrich, I.; Weiß, K.-A.; Dürr, I. Overview of PV module encapsulation materials. *Photovoltaics International* **2013**, *19*, 85-92.
8. Ma, S.; Yuan, G.; Zhang, Y.; Yang, N.; Li, Y.; Chen, Q. Development of encapsulation strategies towards the commercialization of perovskite solar cells. *Energy & Environmental Science* **2022**, *15*, 13-55.
9. Wang, H.; Cheng, X.; Yang, H.; He, W.; Chen, Z.; Xu, L.; Song, D. Potential-induced degradation: Recombination behaviour, temperature coefficients and mismatch losses in crystalline silicon photovoltaic power plant. *Solar Energy* **2019**, *188*, 258-264.

10. Vázquez, M.; Rey-Stolle, I. Photovoltaic module reliability model based on field degradation studies. *Progress in photovoltaics: Research and Applications* **2008**, *16*, 419-433.
11. Daher, D.H.; Gaillard, L.; Ménézo, C. Experimental assessment of long-term performance degradation for a PV power plant operating in a desert maritime climate. *Renewable Energy* **2022**.
12. Wohlgemuth, J. *IEC 61215: What it is and isn't (Presentation)*; National Renewable Energy Lab.(NREL), Golden, CO (United States): 2012.
13. Jordan, D.C.; Sekulic, B.; Marion, B.; Kurtz, S.R. Performance and aging of a 20-year-old silicon PV system. *IEEE Journal of Photovoltaics* **2015**, *5*, 744-751.
14. Han, H.; Dong, X.; Li, B.; Yan, H.; Verlinden, P.J.; Liu, J.; Huang, J.; Liang, Z.; Shen, H. Degradation analysis of crystalline silicon photovoltaic modules exposed over 30 years in hot-humid climate in China. *Solar Energy* **2018**, *170*, 510-519.
15. Ndiaye, A.; Charki, A.; Kobi, A.; Kébé, C.M.F.; Ndiaye, P.A.; Sambou, V. Degradations of silicon photovoltaic modules: A literature review. *Solar Energy* **2013**, *96*, 140-151, doi:10.1016/j.solener.2013.07.005.
16. Triki-Lahiani, A.; Abdelghani, A.B.-B.; Slama-Belkhodja, I. Fault detection and monitoring systems for photovoltaic installations: A review. *Renewable and Sustainable Energy Reviews* **2018**, *82*, 2680-2692.
17. Bai, A.; Popp, J.; Balogh, P.; Gabnai, Z.; Pályi, B.; Farkas, I.; Pintér, G.; Zsiborács, H. Technical and economic effects of cooling of monocrystalline photovoltaic modules under Hungarian conditions. *Renewable and Sustainable Energy Reviews* **2016**, *60*, 1086-1099.
18. Aboagye, B.; Gyamfi, S.; Ofosu, E.A.; Djordjevic, S. Investigation into the impacts of design, installation, operation and maintenance issues on performance and degradation of installed solar photovoltaic (PV) systems. *Energy for Sustainable Development* **2022**, *66*, 165-176, doi:https://doi.org/10.1016/j.esd.2021.12.003.
19. Jordan, D.C.; Kurtz, S.R.; VanSant, K.; Newmiller, J. Compendium of photovoltaic degradation rates. *Progress in Photovoltaics: Research and Applications* **2016**, *24*, 978-989.
20. Köntges, M.; Kurtz, S.; Packard, C.; Jahn, U.; Berger, K.A.; Kato, K.; Friesen, T.; Liu, H.; Van Iseghem, M. Review of failures of photovoltaic modules IEA PVPS Task 13 external final report March 2014. *IEA-PVPS T13-01* **2014**, *2014*.
21. Golive, Y.R.; Zachariah, S.; Dubey, R.; Chattopadhyay, S.; Bhaduri, S.; Singh, H.K.; Bora, B.; Kumar, S.; Tripathi, A.K.; Kottantharayil, A. Analysis of field degradation rates observed in all-India survey of photovoltaic module reliability 2018. *IEEE Journal of Photovoltaics* **2019**, *10*, 560-567.
22. Quansah, D.A.; Adaramola, M.S. Ageing and degradation in solar photovoltaic modules installed in northern Ghana. *Solar Energy* **2018**, *173*, 834-847, doi:10.1016/j.solener.2018.08.021.
23. Olivencia Polo, F.A.; Ferrero Bermejo, J.; Gómez Fernández, J.F.; Crespo Márquez, A. Failure mode prediction and energy forecasting of PV plants to assist dynamic maintenance tasks by ANN based models. *Renewable Energy* **2015**, *81*, 227-238, doi:https://doi.org/10.1016/j.renene.2015.03.023.
24. Sepanski, A.; Reil, F.; Vaaßen, W.; Janknecht, E.; Hupach, U.; Bogdanski, N.; van Heeckeren, B. Assessing Fire Risks in Photovoltaic Systems and Developing Safety Concepts for Risk Minimization. **2018**.
25. Cancelliere, P. PV electrical plants fire risk assessment and mitigation according to the Italian national fire services guidelines. *Fire and Materials* **2016**, *40*, 355-367.
26. Mohd Nizam Ong, N.A.F.; Mohd Tohir, M.Z.; Mutlak, M.M.; Sadiq, M.A.; Omar, R.; Md Said, M.S. BowTie analysis of rooftop grid-connected photovoltaic systems. *Process Safety Progress* **2022**, *41*, S106-S117.
27. Wohlgemuth, J.H.; Kurtz, S.R. How can we make PV modules safer? *2012 38th IEEE Photovoltaic Specialists Conference* **2012**, 003162-003165.
28. Aram, M.; Zhang, X.; Qi, D.; Ko, Y. A State-of-the-Art Review of Fire Safety of Photovoltaic Systems in Buildings. *Journal of Cleaner Production* **2021**, 127239.
29. Blazey, S. Fire and Solar PV Systems–Investigations and Evidence. **2017**.
30. Wu, Z.; Hu, Y.; Wen, J.X.; Zhou, F.; Ye, X. A review for solar panel fire accident prevention in large-scale PV applications. *IEEE Access* **2020**, *8*, 132466-132480.
31. Bansal, N.; Jaiswal, S.P.; Singh, G. Long term operational performance and experimental on-field degradation measurement of 10 MW PV plant in remote location in India. *Energy for Sustainable Development* **2022**, *67*, 135-150, doi:https://doi.org/10.1016/j.esd.2022.01.007.
32. Bansal, N.; Jaiswal, S.P.; Singh, G. Prolonged degradation and reliability assessment of installed modules operational for 10 years in 5 MW PV plant in hot semi-arid climate. *Energy for Sustainable Development* **2022**, *68*, 373-389.

33. Aboagye, B.; Gyamfi, S.; Ofosu, E.A.; Djordjevic, S. CHARACTERISATION OF VISUAL DEFECTS ON INSTALLED SOLAR PHOTOVOLTAIC (PV) MODULES IN DIFFERENT CLIMATIC ZONES IN GHANA. *Scientific African* **2023**, e01682.
34. Colvin, D.J.; Iqbal, N.; Yerger, J.H.; Li, F.; Sinha, A.; Vicnansky, G.; Brummer, G.; Zheng, N.; Schneller, E.J.; Barkaszi, J. Degradation of monocrystalline silicon photovoltaic modules from a 10-year-old rooftop system in Florida. *IEEE Journal of Photovoltaics* **2023**, *13*, 275-282.
35. Chekal Affari, B.; Kahoul, N.; Haouam, A.; Cheghib, H.; Necaibia, A.; Younes, M.; Kherici, Z. Power losses in PV arrays of field-aged modules. *Microelectronics Reliability* **2023**, *147*, 115052, doi:https://doi.org/10.1016/j.microrel.2023.115052.
36. Belhaouas, N.; Mehareb, F.; Kouadri-Boudjelthia, E.; Assem, H.; Bensalem, S.; Hadjrioua, F.; Aissaoui, A.; Hafdaoui, H.; Chahtou, A.; Bakria, K. The performance of solar PV modules with two glass types after 11 years of outdoor exposure under the mediterranean climatic conditions. *Sustainable Energy Technologies and Assessments* **2022**, *49*, 101771.
37. Faye, I.; Ndiaye, A.; Camara, M.; Geke, R.; Blieske, U.; Thiame, M.; Kobor, D. Investigation of Crystalline Silicon Photovoltaic Modules Degradation After 14 years Outdoor Exposure in Cologne Climate (Germany) by Electroluminescence (EL) and Infrared (IR). In Proceedings of the Proceedings of the 52nd American Solar Energy Society National Solar Conference 2023, Cham, 2023//, 2023; pp. 105-113.
38. Segbefia, O.K.; Akhtar, N.; Sætre, T.O. Defects and fault modes of field-aged photovoltaic modules in the Nordics. *Energy Reports* **2023**, *9*, 3104-3119.
39. Segbefia, O.K.; Akhtar, N.; Sætre, T.O. Moisture induced degradation in field-aged multicrystalline silicon photovoltaic modules. *Solar Energy Materials and Solar Cells* **2023**, *258*, 112407, doi:https://doi.org/10.1016/j.solmat.2023.112407.
40. Schulze, K.; Groh, M.; Nieß, M.; Vodermayer, C.; Wotruba, G.; Becker, G. Untersuchung von Alterungseffekten bei monokristallinen PV-Modulen mit mehr als 15 Betriebsjahren durch Elektrolumineszenz-und Leistungsmessung. In Proceedings of the Proc. 28. Symposium Photovoltaische Solarenergie, 2012.
41. Jordan, D.C.; Kurtz, S.R. Photovoltaic degradation rates—an analytical review. *Progress in photovoltaics: Research and Applications* **2013**, *21*, 12-29.
42. Durand, S.; Bowling, D. *Field experience with photovoltaic systems: Ten-year assessment. Final report*; Electric Power Research Inst., Palo Alto, CA (United States); Southwest …: 1993.
43. IEC, I. 60050-191: International electrotechnical vocabulary: Chapter 191: Dependability and quality of service. *International Electrotechnical Commission, Geneva* **1990**.
44. Jordan, D.C.; Silverman, T.J.; Wohlgemuth, J.H.; Kurtz, S.R.; VanSant, K.T. Photovoltaic failure and degradation modes. *Progress in Photovoltaics: Research and Applications* **2017**, *25*, 318-326, doi:10.1002/pip.2866.
45. Jordan, D.; Haegel, N.; Barnes, T. Photovoltaics module reliability for the terawatt age. *Progress in Energy* **2022**.
46. Romero-Fiances, I.; Livera, A.; Theristis, M.; Makrides, G.; Stein, J.S.; Nofuentes, G.; de la Casa, J.; Georghiou, G.E. Impact of duration and missing data on the long-term photovoltaic degradation rate estimation. *Renewable Energy* **2022**, *181*, 738-748.
47. Heywang, W.; Zaininger, K.H. Silicon: the semiconductor material. In *Silicon*; Springer: 2004; pp. 25-42.
48. Kılıç, A.; Öztürk, A. *Güneş enerjisi*; Kipaş Dağıtımcılık: 1983.
49. Gürtürk, M.; Benli, H.; Ertürk, N.K. Determination of the effects of temperature changes on solar glass used in photovoltaic modules. *Renewable Energy* **2020**, *145*, 711-724.
50. Afridi, M.; Kumar, A.; ibne Mahmood, F.; Tamizhmani, G. Hotspot testing of glass/backsheet and glass/glass PV modules pre-stressed in extended thermal cycling. *Solar Energy* **2023**, *249*, 467-475.
51. Tsanakas, J.A.; Ha, L.; Buerhop, C. Faults and infrared thermographic diagnosis in operating c-Si photovoltaic modules: A review of research and future challenges. *Renewable and Sustainable Energy Reviews* **2016**, *62*, 695-709, doi:10.1016/j.rser.2016.04.079.
52. Enaganti, P.K.; Bhattacharjee, A.; Ghosh, A.; Chanchangi, Y.N.; Chakraborty, C.; Mallick, T.K.; Goel, S. Experimental investigations for dust build-up on low-iron glass exterior and its effects on the performance of solar PV systems. *Energy* **2022**, *239*, 122213.
53. Tagawa, K.; Kutani, A.; Qinglin, P. Effect of sand erosion of glass surface on performances of photovoltaic module. *Proceedings of the Sustainable Research and Innovation Conference* **2022**, 75-77.

54. King, D.; Quintana, M.; Kratochvil, J.; Ellibee, D.; Hansen, B. Photovoltaic module performance and durability following long-term field exposure. *Progress in Photovoltaics: research and applications* **2000**, *8*, 241-256.
55. King, D.; Pern, F.; Pitts, J.; Bingham, C.; Czanderna, A. Optical changes in cerium-containing glass as a result of accelerated exposure testing [of PV modules]. In Proceedings of the Conference Record of the Twenty Sixth IEEE Photovoltaic Specialists Conference-1997, 1997; pp. 1117-1120.
56. Kempe, M.D.; Moricone, T.; Kilkenny, M. Effects of cerium removal from glass on photovoltaic module performance and stability. In Proceedings of the Reliability of Photovoltaic Cells, Modules, Components, and Systems II, 2009; p. 74120Q.
57. Hossion, M.A. Visual and electrical degradation data of five years aged rooftop photovoltaic modules. *Data in Brief* **2020**, *31*, 105762, doi:https://doi.org/10.1016/j.dib.2020.105762.
58. Quansah, D.A.; Adaramola, M.S. Comparative study of performance degradation in poly- and mono-crystalline-Si solar PV modules deployed in different applications. *International Journal of Hydrogen Energy* **2018**, *43*, 3092-3109, doi:10.1016/j.ijhydene.2017.12.156.
59. Dietrich, S.; Pander, M.; Ebert, M.; Bagdahn, J. Mechanical assessment of large photovoltaic modules by test and finite element analysis. In Proceedings of the 23rd European Photovoltaic Solar Energy Conference. Valencia, Spain, 2008.
60. Cavieres, R.; Barraza, R.; Estay, D.; Bilbao, J.; Valdivia-Lefort, P. Automatic soiling and partial shading assessment on PV modules through RGB images analysis. *Applied Energy* **2022**, *306*, 117964.
61. Bora, B.; Sastry, O.S.; Kumar, R.; Dubey, R.; Chattopadhyay, S.; Vasi, J.; Mondal, S.; Prasad, B. Failure mode analysis of PV modules in different climatic conditions. *IEEE Journal of Photovoltaics* **2020**, *11*, 453-460.
62. Chandel, S.S.; Nagaraju Naik, M.; Sharma, V.; Chandel, R. Degradation analysis of 28 year field exposed mono-c-Si photovoltaic modules of a direct coupled solar water pumping system in western Himalayan region of India. *Renewable Energy* **2015**, *78*, 193-202, doi:10.1016/j.renene.2015.01.015.
63. Băjenescu, T.-M.I. Some reliability aspects of photovoltaic modules. In *Reliability and Ecological Aspects of Photovoltaic Modules*; IntechOpen: 2020.
64. Castaner, L.; Silvestre, S. *Modelling photovoltaic systems using PSpice*; John Wiley and Sons: 2002.
65. Deng, S.; Zhang, Z.; Ju, C.; Dong, J.; Xia, Z.; Yan, X.; Xu, T.; Xing, G. Research on hot spot risk for high-efficiency solar module. *Energy Procedia* **2017**, *130*, 77-86.
66. Meyer, E.L.; Van Dyk, E.E. The effect of reduced shunt resistance and shading on photovoltaic module performance. In Proceedings of the Conference Record of the Thirty-first IEEE Photovoltaic Specialists Conference, 2005., 2005; pp. 1331-1334.
67. Vankadara, S.K.; Chatterjee, S.; Balachandran, P.K. An accurate analytical modeling of solar photovoltaic system considering Rs and Rsh under partial shaded condition. *International Journal of System Assurance Engineering and Management* **2022**, 1-10.
68. Ghanbari, T. Permanent partial shading detection for protection of photovoltaic panels against hot spotting. *IET Renewable Power Generation* **2016**, *11*, 123-131.
69. Jadin, M.S.b.; Safian, S.F.A.; Ghazali, K.H.; Ven, T.L.; Shah, A.S.M. Hotspot Detection in Photovoltaic Array Using Thermal Imaging Method. *Proceedings of the 6th International Conference on Electrical, Control and Computer Engineering* **2022**, 101-107.
70. Hasan, O.; Arif, A. Performance and life prediction model for photovoltaic modules: Effect of encapsulant constitutive behavior. *Solar energy materials and solar cells* **2014**, *122*, 75-87.
71. Miller, D.C.; Bokria, J.G.; Burns, D.M.; Fowler, S.; Gu, X.; Hacke, P.L.; Honeker, C.C.; Kempe, M.D.; Köhl, M.; Phillips, N.H. Degradation in photovoltaic encapsulant transmittance: Results of the first PVQAT TG5 artificial weathering study. *Progress in Photovoltaics: Research and Applications* **2019**, *27*, 391-409.
72. López-Escalante, M.; Caballero, L.J.; Martín, F.; Gabás, M.; Cuevas, A.; Ramos-Barrado, J. Polyolefin as PID-resistant encapsulant material in PV modules. *Solar Energy Materials and Solar Cells* **2016**, *144*, 691-699.
73. Kempe, M. Overview of scientific issues involved in selection of polymers for PV applications. In Proceedings of the 2011 37th IEEE Photovoltaic Specialists Conference, 2011; pp. 000085-000090.
74. Habersberger, B.M.; Hacke, P.; Madenjian, L.S. Evaluation of the PID-s susceptibility of modules encapsulated in materials of varying resistivity. In Proceedings of the 2018 IEEE 7th World Conference on Photovoltaic Energy Conversion (WCPEC)(A Joint Conference of 45th IEEE PVSC, 28th PVSEC & 34th EU PVSEC), 2018; pp. 3807-3809.

75. Kapur, J.; Stika, K.M.; Westphal, C.S.; Norwood, J.L.; Hamzavytehrany, B. Prevention of potential-induced degradation with thin ionomer film. *IEEE Journal of Photovoltaics* **2014**, *5*, 219-223.
76. Azam, M.F.; Shahzad, N.; Rafique, A.; Ayub, M.; Khalid, H.A.; Waqas, A. Accelerated UV stress testing and characterization of PV-modules: Reliability analysis using different encapsulants and glass sheets. *Sustainable Energy Technologies and Assessments* **2023**, *56*, 103119.
77. Peike, C.; Purschke, L.; Weiss, K.-A.; Köhl, M.; Kempe, M. Towards the origin of photochemical EVA discoloration. In Proceedings of the 2013 IEEE 39th Photovoltaic Specialists Conference (PVSC), 2013; pp. 1579-1584.
78. Kyranaki, N.; Smith, A.; Yendall, K.; Hutt, D.A.; Whalley, D.C.; Gottschalg, R.; Betts, T.R. Damp-heat induced degradation in photovoltaic modules manufactured with passivated emitter and rear contact solar cells. *Progress in Photovoltaics: Research and Applications*.
79. Badiee, A.; Ashcroft, I.; Wildman, R.D. The thermo-mechanical degradation of ethylene vinyl acetate used as a solar panel adhesive and encapsulant. *International Journal of Adhesion and Adhesives* **2016**, *68*, 212-218.
80. Desai, U.; Sharma, B.K.; Singh, A.; Singh, A. A comparison of evolution of adhesion mechanisms and strength post damp-heat aging for a range of VA content in EVA encapsulant with photovoltaic backsheet. *Solar Energy* **2022**, *231*, 908-920.
81. Lathrop, J.W.; Hartman, R.A.; Saylor, C.R. Investigation of reliability attributes and accelerated stress factors on terrestrial solar cells. **1981**.
82. Bansal, N.; Jaiswal, S.P.; Singh, G. Comparative investigation of performance evaluation, degradation causes, impact and corrective measures for ground mount and rooftop solar PV plants–A review. *Sustainable Energy Technologies and Assessments* **2021**, *47*, 101526.
83. Manganiello, P.; Balato, M.; Vitelli, M. A survey on mismatching and aging of PV modules: The closed loop. *IEEE Transactions on Industrial Electronics* **2015**, *62*, 7276-7286.
84. Stark, W.; Jaunich, M. Investigation of Ethylene/Vinyl Acetate Copolymer (EVA) by thermal analysis DSC and DMA. *Polymer Testing* **2011**, *30*, 236-242.
85. Gok, A.; Gordon, D.A.; Wang, M.; French, R.H.; Bruckman, L.S. Degradation Science and Pathways in PV Systems. In *Durability and Reliability of Polymers and Other Materials in Photovoltaic Modules*; Elsevier: 2019; pp. 47-93.
86. Perret-Aebi, L.E.; Li, H.Y.; Théron, R.; Roeder, G.; Luo, Y.; Turlings, T.; Lange, R.F.M.; Ballif, C. Insights on EVA lamination process: Where do the Bubbles Come From. *25th European Photovoltaic Solar Energy Conference and Exhibition, Valencia, Spain* **2010**.
87. Karthikeyan, S.; Ajay, G.B.; Ahamed, N.R.; Sharun, A. Edge AI–Based Aerial Monitoring. *Applied Edge AI: Concepts, Platforms, and Industry Use Cases* **2022**, 237.
88. Shrestha, S.M.; Mallineni, J.K.; Yedidi, K.R.; Knisely, B.; Tatapudi, S.; Kuitche, J.; TamizhMani, G. Determination of dominant failure modes using FMECA on the field deployed c-Si modules under hot-dry desert climate. *IEEE journal of photovoltaics* **2014**, *5*, 174-182.
89. Rajput, P.; Tiwari, G.N.; Sastry, O.S.; Bora, B.; Sharma, V. Degradation of mono-crystalline photovoltaic modules after 22 years of outdoor exposure in the composite climate of India. *Solar Energy* **2016**, *135*, 786-795.
90. de Oliveira, M.C.C.; Cardoso, A.S.A.D.; Viana, M.M.; Lins, V.d.F.C. The causes and effects of degradation of encapsulant ethylene vinyl acetate copolymer (EVA) in crystalline silicon photovoltaic modules: A review. *Renewable and Sustainable Energy Reviews* **2018**, *81*, 2299-2317.
91. Frederick, J.; Snell, H.; Haywood, E. Solar ultraviolet radiation at the earth's surface. *Photochemistry and Photobiology* **1989**, *50*, 443-450.
92. Klampaftis, E.; Congiu, M.; Robertson, N.; Richards, B.S. Luminescent ethylene vinyl acetate encapsulation layers for enhancing the short wavelength spectral response and efficiency of silicon photovoltaic modules. *IEEE Journal of Photovoltaics* **2011**, *1*, 29-36.
93. Kamel, M.S.A.; Oelgemöller, M.; Jacob, M.V. Sustainable plasma polymer encapsulation materials for organic solar cells. *Journal of Materials Chemistry A* **2022**, *10*, 4683-4694.
94. Cristofoli, K. Preparação e caracterização de filmes de PEBD aditivados com fotoestabilizantes para a proteção de espumantes rose. **2014**.
95. Holley, W.H.; Agro, S.C.; Galica, J.P.; Thoma, L.A.; Yorgensen, R.S.; Ezrin, M.; Klemchuk, P.; Lavigne, G. Investigation into the causes of browning in EVA encapsulated flat plate PV modules. In Proceedings of

the Proceedings of 1994 IEEE 1st World Conference on Photovoltaic Energy Conversion-WCPEC (A Joint Conference of PVSC, PVSEC and PSEC), 1994; pp. 893-896.

96. Jiang, S.; Wang, K.; Zhang, H.; Ding, Y.; Yu, Q. Encapsulation of PV modules using ethylene vinyl acetate copolymer as the encapsulant. *Macromolecular Reaction Engineering* **2015**, *9*, 522-529.
97. Noman, M.; Tu, S.; Ahmad, S.; Zafar, F.U.; Khan, H.A.; Rehman, S.U.; Waqas, M.; Khan, A.D.; Rehman, O.u. Assessing the reliability and degradation of 10–35 years field-aged PV modules. *Plos one* **2022**, *17*, e0261066.
98. Arularasu, P. Combined UV-temperature-humidity Accelerated Testing of PV Modules: Reliability of UV-cut and UV-pass EVA Encapsulants. Arizona State University, 2019.
99. ISO, Standard 17223 "Plastics - Determination of yellowness index and change in yellowness index" (2014). .
100. de Oliveira, M.C.C.; Cassini, D.A.; Diniz, A.S.A.C.; Soares, L.G.; Viana, M.M.; Kazmerski, L.L.; Lins, V.d.F.C. Comparison and analysis of performance and degradation differences of crystalline-Si photovoltaic modules after 15-years of field operation. *Solar Energy* **2019**, *191*, 235-250.
101. Yong, H.; Minemoto, T.; Takahashi, T. Dependence of Photovoltage on Incident Photon Energies Investigated by Photo-assisted Kelvin Probe Force Microscopy on Cu (In, Ga) Se 2 Solar Cells. In Proceedings of the 2018 IEEE 7th World Conference on Photovoltaic Energy Conversion (WCPEC)(A Joint Conference of 45th IEEE PVSC, 28th PVSEC & 34th EU PVSEC), 2018; pp. 1966-1969.
102. Adothu, B.; Chattopadhyay, S.; Bhatt, P.; Hui, P.; Costa, F.R.; Mallick, S. Early-stage identification of encapsulants photobleaching and discoloration in crystalline silicon photovoltaic module laminates. *Progress in Photovoltaics: Research and Applications*.
103. Kaplani, E. Detection of degradation effects in field-aged c-Si solar cells through IR thermography and digital image processing. *International Journal of Photoenergy* **2012**, *2012*.
104. Kurtz, S. Photovoltaic Module Reliability Workshop 2014: February 25-26, 2014. **2014**.
105. Ferrara, C.; Philipp, D. Why Do PV Modules Fail? *Energy Procedia* **2012**, *15*, 379-387, doi:10.1016/j.egypro.2012.02.046.
106. Rosillo, F.; Alonso-Garcia, M. Evaluation of color changes in PV modules using reflectance measurements. *Solar Energy* **2019**, *177*, 531-537.
107. Pern, F.; Czanderna, A.; Emery, K.; Dhere, R. Weathering degradation of EVA encapsulant and the effect of its yellowing on solar cell efficiency. In Proceedings of the The Conference Record of the Twenty-Second IEEE Photovoltaic Specialists Conference-1991, 1991; pp. 557-561.
108. Dechthummarong, C.; Wiengmoon, B.; Chenvidhya, D.; Jivacate, C.; Kirtikara, K. Physical deterioration of encapsulation and electrical insulation properties of PV modules after long-term operation in Thailand. *Solar energy materials and solar cells* **2010**, *94*, 1437-1440.
109. Photovoltaic, C.S.T. Modules—Design Qualification and Type Approval. *IEC* **2005**, *1215*, 2005-2005.
110. Diniz, A.S.A.; Cassini, D.A.; de Oliveira, M.C.; de Lins, V.F.; Viana, M.M.; Braga, D.S.; Kazmerski, L.L. Evaluation of Performance Losses and Degradation of Aged Crystalline Si Photovoltaic Modules Installed in Minas Gerais (Brazil). In *Renewable Energy and Sustainable Buildings*; Springer: 2020; pp. 29-46.
111. Dhimish, M. Micro cracks distribution and power degradation of polycrystalline solar cells wafer: Observations constructed from the analysis of 4000 samples. *Renewable Energy* **2020**, *145*, 466-477, doi:https://doi.org/10.1016/j.renene.2019.06.057.
112. Eslami Majd, A.; Ekere, N.N. Crack initiation and growth in PV module interconnection. *Solar Energy* **2020**, *206*, 499-507, doi:https://doi.org/10.1016/j.solener.2020.06.036.
113. Grunow, P.; Clemens, P.; Hoffmann, V.; Litzenburger, B.; Podlowski, L. Influence of micro cracks in multi-crystalline silicon solar cells on the reliability of PV modules. *Proceedings of the 20th EUPVSEC* **2005**, 2042-2047.
114. BrightSpot Automation, L.L.C.; Westford, M.A. Solar panel design factors to reduce the impact of cracked cells and the tendency for crack propagation. *NREL PV Module Reliability Workshop, Denver, CO USA* **2015**.
115. Sander, M.; Dietrich, S.; Pander, M.; Schweizer, S.; Ebert, M.; Bagdahn, J. Investigations on crack development and crack growth in embedded solar cells. *Reliability of Photovoltaic Cells, Modules, Components, and Systems IV* **2011**, *8112*, 811209.
116. Buerhop, C.; Schlegel, D.; Vodermayer, C.; Nieß, M. Quality control of PV-modules in the field using infrared-thermography. In Proceedings of the 26th European Photovoltaic Solar Energy Conference, 2011; pp. 3894-3897.

117. Siruvuri, S.V.; Budarapu, P.R.; Paggi, M. Influence of cracks on fracture strength and electric power losses in Silicon solar cells at high temperatures: deep machine learning and molecular dynamics approach. *Applied Physics A* **2023**, *129*, 408.
118. Dhimish, M.; Holmes, V.; Mehrdadi, B.; Dales, M. The impact of cracks on photovoltaic power performance. *Journal of Science: Advanced Materials and Devices* **2017**, *2*, 199-209.
119. Sohail, A.; Ul Islam, N.; Ul Haq, A.; Ul Islam, S.; Shafi, I.; Park, J. Fault detection and computation of power in PV cells under faulty conditions using deep-learning. *Energy Reports* **2023**, *9*, 4325-4336, doi:https://doi.org/10.1016/j.egyr.2023.03.094.
120. Dolara, A.; Leva, S.; Manzolini, G.; Ogliari, E. Investigation on performance decay on photovoltaic modules: Snail trails and cell microcracks. *IEEE journal of photovoltaics* **2014**, *4*, 1204-1211.
121. Sinaga, R. Turnitin: A preliminary study of common defects of photovoltaic modules in West Timor, Indonesia. **2023**.
122. Duerr, I.; Bierbaum, J.; Metzger, J.; Richter, J.; Philipp, D. Silver Grid Finger Corrosion on Snail Track affected PV Modules – Investigation on Degradation Products and Mechanisms. *Energy Procedia* **2016**, *98*, 74-85, doi:10.1016/j.egypro.2016.10.083.
123. Swanson, R.; Cudzinovic, M.; DeCeuster, D.; Desai, V.; Jürgens, J.; Kaminar, N.; Mulligan, W.; Rodrigues-Barbarosa, L.; Rose, D.; Smith, D. The surface polarization effect in high-efficiency silicon solar cells. *15th PVSEC* **2005**.
124. Köntges, M.; Kurtz, S.; Packard, C.; Jahn, U.; Berger, K.A.; Kato, K.; Friesen, T.; Liu, H.; Van Iseghem, M.; Wohlgemuth, J. Review of failures of photovoltaic modules. **2014**.
125. Dhimish, M.; Tyrrell, A.M. Power loss and hotspot analysis for photovoltaic modules affected by potential induced degradation. *npj Materials Degradation* **2022**, *6*, 1-8.
126. Yamaguchi, S.; Masuda, A.; Marumoto, K.; Ohdaira, K. Mechanistic Understanding of Polarization-Type Potential-Induced Degradation in Crystalline-Silicon Photovoltaic Cell Modules. *Advanced Energy and Sustainability Research* **2023**, *4*, 2200167.
127. Köntges, M.; Oreski, G.; Jahn, U.; Herz, M.; Hacke, P.; Weiß, K.-A. *Assessment of Photovoltaic Module Failures in the Field: International Energy Agency Photovoltaic Power Systems Programme: IEA PVPS Task 13, Subtask 3: Report IEA-PVPS T13-09: 2017*; International Energy Agency: 2017.
128. Pingel, S.; Janke, S.; Frank, O. Recovery methods for modules affected by potential induced degradation (PID). *27th European Photovoltaic Solar Energy Conference and Exhibition (Frankfurt)* **2012**, 3379-3383.
129. Molto, C.; Oh, J.; Mahmood, F.I.; Li, M.; Hacke, P.; Li, F.; Smith, R.; Colvin, D.; Matam, M.; DiRubio, C. Review of Potential-Induced Degradation in Bifacial Photovoltaic Modules. *Energy Technology* **2023**, *11*, 2200943.
130. Gallardo-Saavedra, S.; Hernández-Callejo, L.; del Carmen Alonso-García, M.; Santos, J.D.; Morales-Aragonés, J.I.; Alonso-Gómez, V.; Moretón-Fernández, Á.; González-Rebollo, M.Á.; Martínez-Sacristán, O. Nondestructive characterization of solar PV cells defects by means of electroluminescence, infrared thermography, I–V curves and visual tests: Experimental study and comparison. *Energy* **2020**, *205*, 117930.
131. Köntges, M.; Kajari-Schröder, S.; Kunze, I. Cell cracks measured by UV fluorescence in the field. *Proceedings of the 27th EU PVSEC, Frankfurt, Germany* **2012**, 3033-3040.
132. Colvin, D.J.; Schneller, E.J.; Davis, K.O. Impact of interconnection failure on photovoltaic module performance. *Progress in Photovoltaics: Research and Applications* **2021**, *29*, 524-532.
133. Majd, A.E.; Ekere, N.N.; Darvazi, A.R.; Sedehi, A.A. Creep-fatigue lifetime estimation of efficient photovoltaic module ribbon interconnections. *Microelectronics Reliability* **2022**, *139*, 114831.
134. Köntges, M.; Altmann, S.; Heimberg, T.; Jahn, U.; Berger, K.A. Mean degradation rates in PV systems for various kinds of PV module failures. *Proceedings of the 32nd European Photovoltaic Solar Energy Conference and Exhibition, Munich, Germany* **2016**, 21-24.
135. Kurtz, S. 2017 NREL Photovoltaic Reliability Workshop. **2017**.
136. Illya, G.; Handara, V.; Siahandan, M.; Nathania, A.; Budiman, A.S. Mechanical Studies of Solar Photovoltaics (PV) Backsheets Under Salt Damp Heat Environments. *Procedia Engineering* **2017**, *215*, 238-245, doi:https://doi.org/10.1016/j.proeng.2017.12.144.
137. Oreski, G.; Barretta, C.; Macher, A.; Eder, G.; Neumaier, L.; Feichtner, M.; Aarnio Winterhof, M. Investigation of the Crack Propensity of Co-Extruded Polypropylene Backsheet Films for Photovoltaic Modules. *Available at SSRN 4416009* **2023**.

138. Elfaqih, A.K.; Tawil, I.H. Mechanical behavior study of PPCF material as solar photovoltaic backsheet. 2022; pp. 650-654.
139. Pascual, J.; García, M.; Marcos, J.; Marroyo, L. Analysis of polyamide and fluoropolymer backsheets: Degradation and insulation failure in field-aged photovoltaic modules. *Progress in Photovoltaics: Research and Applications* **2023**, *31*, 494-505.
140. Gebhardt, P.; Bauermann, L.P.; Philipp, D. Backsheet chalking—theoretical background and relation to backsheet cracking and insulation failures. 2018; pp. 24-28.
141. Uličná, S.; Owen-Bellini, M.; Moffitt, S.L.; Sinha, A.; Tracy, J.; Roy-Choudhury, K.; Miller, D.C.; Hacke, P.; Schelhas, L.T. A study of degradation mechanisms in PVDF-based photovoltaic backsheets. *Scientific Reports* **2022**, *12*, 14399.
142. Xia, J.; Liu, Y.; Hu, H.; Zhu, X.; Lv, H.; Phillips, N.H.; Choudhury, K.R.; Gambogi, W.J.; Rodriguez, M.; Simon, E.S. Impact of specimen preparation method on photovoltaic backsheet degradation during accelerated aging test. *Energy Science & Engineering* **2022**, *10*, 1961-1971.
143. Mühleisen, W. Minimizing Crack Propagation in Cracked PV Backsheets with Repair Coatings. **2022**.
144. Beaucarne, G.; Eder, G.; Jadot, E.; Voronko, Y.; Mühleisen, W. Repair and preventive maintenance of photovoltaic modules with degrading backsheets using flowable silicone sealant. *Progress in Photovoltaics: Research and Applications* **2022**, *30*, 1045-1053.
145. Wu, Z.; Lyu, S.; Peng, Q.; Han, H.; Zhu, D. Thermomechanical Stress Distribution Analysis of Junction Box on Silicon Photovoltaic Modules Based on Finite Element Analysis. *IEEE Journal of Photovoltaics* **2019**, *9*, 1716-1720, doi:10.1109/JPHOTOV.2019.2940530.
146. Diaz-Dorado, E.; Suárez-García, A.; Carrillo, C.; Cidras, J. Influence of the shadows in photovoltaic systems with different configurations of bypass diodes. In Proceedings of the SPEEDAM 2010, 2010; pp. 134-139.
147. Bakır, H. A comparative evaluation and real-time measurement of failures in solar power plants by thermal imaging in Turkey. *Thermal Science and Engineering Progress* **2023**, *42*, 101945, doi:https://doi.org/10.1016/j.tsep.2023.101945.
148. Kim, M.-S.; Kim, D.-H.; Kim, H.-J.; Prabakar, K. A Novel Strategy for Monitoring a PV Junction Box Based on LoRa in a 3 kW Residential PV System. *Electronics* **2022**, *11*, 709.
149. Brecl, K.; Pirc, M.; Bokalič, M.; Morelj, D.; Topič, M. PV module behaviour on the substring level under real conditions monitored by junction box electronic device Jubomer. *IET Renewable Power Generation* **2019**, *13*, 2802-2806.
150. Ong, N.A.F.M.N.; Sadiq, M.A.; Said, M.S.M.; Jomaas, G.; Tohir, M.Z.M.; Kristensen, J.S. Fault tree analysis of fires on rooftops with photovoltaic systems. *Journal of Building Engineering* **2022**, *46*, 103752.
151. Daher, D.H.; Aghaei, M.; Quansah, D.A.; Adaramola, M.S.; Parvin, P.; Ménézo, C. Multi-pronged degradation analysis of a photovoltaic power plant after 9.5 years of operation under hot desert climatic conditions. *Progress in Photovoltaics: Research and Applications* **2023**.
152. Vo, T.T.E.; Ko, H.; Huh, J.; Park, N. Overview of possibilities of solar floating photovoltaic systems in the offshore industry. *Energies* **2021**, *14*, 6988.
153. Ghosh, A. A comprehensive review of water based PV: Flotavoltaics, under water, offshore & canal top. *Ocean Engineering* **2023**, *281*, 115044, doi:https://doi.org/10.1016/j.oceaneng.2023.115044.
154. Tabet, S.; Ihaddadene, R.; Guerira, B.; Ihaddadene, N. Impact of Dust and Degradation on the Electrical Properties of PV Panels. *Journal of Renewable Energy and Environment* **2023**.
155. Xue-Yan, L.; Ji-Gao, Z. Dust corrosion. In Proceedings of the Proceedings of the 50th IEEE Holm Conference on Electrical Contacts and the 22nd International Conference on Electrical Contacts Electrical Contacts, 2004., 23-23 Sept. 2004, 2004; pp. 255-262.
156. Karimi, M.; Samet, H.; Ghanbari, T.; Moshksar, E. A current based approach for hotspot detection in photovoltaic strings. *International Transactions on Electrical Energy Systems* **2020**, *30*, e12517.
157. Kim, K.A.; Krein, P.T. Hot spotting and second breakdown effects on reverse IV characteristics for mono-crystalline Si photovoltaics. In Proceedings of the 2013 IEEE Energy Conversion Congress and Exposition, 2013; pp. 1007-1014.
158. AE-Solar. SMART MODULES WITH HOT-SPOT FREE TECHNOLOGY. **2018**.
159. Ross, R.G. PV reliability development lessons from JPL's flat plate solar array project. *IEEE Journal of Photovoltaics* **2013**, *4*, 291-298.
160. Oufettoul, H.; Motahhir, S.; Aniba, G.; Masud, M.; AlZain, M.A. Improved TCT topology for shaded photovoltaic arrays. *Energy Reports* **2022**, *8*, 5943-5956.

161. Spanoche, S.A.; Stewart, J.D.; Hawley, S.L.; Opris, I.E. Model-based method for partially shaded PV modules hot spot suppression. *2012 IEEE 38th photovoltaic specialists conference (PVSC) PART 2* **2012**, 1-7.
162. Herrmann, W.; Wiesner, W.; Vaassen, W. Hot spot investigations on PV modules-new concepts for a test standard and consequences for module design with respect to bypass diodes. In Proceedings of the Conference Record of the Twenty Sixth IEEE Photovoltaic Specialists Conference-1997, 1997; pp. 1129-1132.
163. Bakır, H. Detection of Faults in Photovoltaic Modules of SPPS in Turkey; Infrared Thermographic Diagnosis and Recommendations. *Journal of Electrical Engineering & Technology* **2023**, *18*, 1945-1957.
164. Ghosh, S.; Singh, S.K.; Yadav, V.K. Experimental investigation of hotspot phenomenon in PV arrays under mismatch conditions. *Solar Energy* **2023**, *253*, 219-230.
165. Al Mahdi, H.A.; Leahy, P.G.; Morrison, A.P. Predicting Early EVA Degradation in Photovoltaic Modules From Short Circuit Current Measurements. *IEEE Journal of Photovoltaics* **2021**, *11*, 1188-1196.
166. Kuitche, J.M.; Pan, R.; TamizhMani, G. Investigation of Dominant Failure Mode(s) for Field-Aged Crystalline Silicon PV Modules Under Desert Climatic Conditions. *IEEE Journal of Photovoltaics* **2014**, *4*, 814-826, doi:10.1109/JPHOTOV.2014.2308720.
167. Hong, Y.-Y.; Pula, R.A. Methods of photovoltaic fault detection and classification: A review. *Energy Reports* **2022**, *8*, 5898-5929.
168. Tanaka, K.; Matsumoto, K.i.; Keeley, A.R.; Managi, S. The impact of weather changes on the supply and demand of electric power and wholesale prices of electricity in Germany. *Sustainability Science* **2022**, *17*, 1813-1825.
169. Tripathi, A.K.; Aruna, M.; Murthy, C.S.N. Output power loss of photovoltaic panel due to dust and temperature. *International Journal of Renewable Energy Research* **2017**, *7*, 439-442.
170. Hasan, K.; Yousuf, S.B.; Tushar, M.S.H.K.; Das, B.K.; Das, P.; Islam, M.S. Effects of different environmental and operational factors on the PV performance: A comprehensive review. *Energy Science & Engineering* **2022**, *10*, 656-675.
171. Santhakumari, M.; Sagar, N. A review of the environmental factors degrading the performance of silicon wafer-based photovoltaic modules: Failure detection methods and essential mitigation techniques. *Renewable and Sustainable Energy Reviews* **2019**, *110*, 83-100, doi:10.1016/j.rser.2019.04.024.
172. Abdallah, A.A.; Ali, K.; Kivambe, M.M.; Darussalam, B. Common failure modes observed in PV system installed in desert climate.
173. Zaihidee, F.M.; Mekhilef, S.; Seyedmahmoudian, M.; Horan, B. Dust as an unalterable deteriorative factor affecting PV panel's efficiency: Why and how. *Renewable and Sustainable Energy Reviews* **2016**, *65*, 1267-1278.
174. Saidan, M.; Albaali, A.G.; Alasis, E.; Kaldellis, J.K. Experimental study on the effect of dust deposition on solar photovoltaic panels in desert environment. *Renewable Energy* **2016**, *92*, 499-505.
175. Mehmood, U.; Al-Sulaiman, F.A.; Yilbas, B. Characterization of dust collected from PV modules in the area of Dhahran, Kingdom of Saudi Arabia, and its impact on protective transparent covers for photovoltaic applications. *Solar Energy* **2017**, *141*, 203-209.
176. Fan, S.; Wang, Y.; Cao, S.; Sun, T.; Liu, P. A novel method for analyzing the effect of dust accumulation on energy efficiency loss in photovoltaic (PV) system. *Energy* **2021**, 121112.
177. Said, S.A.M.; Walwil, H.M. Fundamental studies on dust fouling effects on PV module performance. *Solar Energy* **2014**, *107*, 328-337.
178. Sayigh, A.; Al-Jandal, S.; Ahmed, H. Dust effect on solar flat surfaces devices in Kuwait. In Proceedings of the Proceedings of the workshop on the physics of non-conventional energy sources and materials science for energy, 1985; pp. 353-367.
179. Elminir, H.K.; Ghitas, A.E.; Hamid, R.; El-Hussainy, F.; Beheary, M.; Abdel-Moneim, K.M. Effect of dust on the transparent cover of solar collectors. *Energy conversion and management* **2006**, *47*, 3192-3203.
180. Kazem, H.A.; Chaichan, M.T.; Al-Waeli, A.H.A.; Al-Badi, R.; Fayad, M.A.; Gholami, A. Dust impact on photovoltaic/thermal system in harsh weather conditions. *Solar Energy* **2022**, *245*, 308-321, doi:https://doi.org/10.1016/j.solener.2022.09.012.
181. Yazdani, H.; Yaghoubi, M. Dust deposition effect on photovoltaic modules performance and optimization of cleaning period: A combined experimental–numerical study. *Sustainable Energy Technologies and Assessments* **2022**, *51*, 101946, doi:https://doi.org/10.1016/j.seta.2021.101946.
182. Sharif, M.A.; Rashid, M.; Korkmaz, F. Effects of Weather and Environmental Conditions on the Power Productivity of Photovoltaic Module in Kirkuk City. *NTU Journal of Renewable Energy* **2023**, *4*, 1-6.

183. Fu, X.; Wang, X.; Gong, Y.; Wang, Y.; Zhang, Y. Impact of Snow Weather on PV Power Generation and Improvement of Power Forecasting. In Proceedings of the 2023 International Conference on Power Energy Systems and Applications (ICoPESA), 24-26 Feb. 2023, 2023; pp. 448-453.
184. Bahanni, C.; Adar, M.; Boulmrharj, S.; Khaidar, M.; Mabrouki, M. Performance comparison and impact of weather conditions on different photovoltaic modules in two different cities. *Indones. J. Electr. Eng. Comput. Sci* **2022**, *25*, 1275-1286.
185. Madeti, S.R.; Singh, S. A comprehensive study on different types of faults and detection techniques for solar photovoltaic system. *Solar Energy* **2017**, *158*, 161-185.
186. Pillai, D.S.; Rajasekar, N. A comprehensive review on protection challenges and fault diagnosis in PV systems. *Renewable and Sustainable Energy Reviews* **2018**, *91*, 18-40.
187. Mellit, A.; Tina, G.M.; Kalogirou, S.A. Fault detection and diagnosis methods for photovoltaic systems: A review. *Renewable and Sustainable Energy Reviews* **2018**, *91*, 1-17.
188. Standard, I.E.C. 61215 Crystalline Silicon Terrestrial Photovoltaic (PV) ModulesDesign Qualification and Type Approval. *International Electrotechnical Commission* **1995**.
189. Kumar, N.M.; Sudhakar, K.; Samykano, M.; Jayaseelan, V. On the technologies empowering drones for intelligent monitoring of solar photovoltaic power plants. *Procedia computer science* **2018**, *133*, 585-593.
190. Buerhop, C.; Bommes, L.; Schlipf, J.; Pickel, T.; Fladung, A.; Peters, M. Infrared imaging of photovoltaic modules A review of the state of the art and future challenges facing gigawatt photovoltaic power stations. *Progress in Energy* **2022**.
191. Goodarzi, D.M.; Lauri, J.; Putaala, J.; Nousiainen, O.; Fabritius, T. Eddy current soldering of solar cell ribbons under a layer of glass. *Solar Energy Materials and Solar Cells* **2023**, *259*, 112427.
192. Drabczyk, K.; Kulesza-Matlak, G.; Drygała, A.; Szindler, M.; Lipiński, M. Electroluminescence imaging for determining the influence of metallization parameters for solar cell metal contacts. *Solar Energy* **2016**, *126*, 14-21.
193. Hobbs, W.; Lavrova, O.; Lockridge, B. *Comparison of Electroluminescence Image Capture Methods*; Sandia National Lab.(SNL-NM), Albuquerque, NM (United States): 2016.
194. Høiaas, I.; Grujic, K.; Imenes, A.G.; Burud, I.; Olsen, E.; Belbachir, N. Inspection and condition monitoring of large-scale photovoltaic power plants: A review of imaging technologies. *Renewable and Sustainable Energy Reviews* **2022**, *161*, 112353.
195. Kajari-Schröder, S.; Kunze, I.; Eitner, U.; Köntges, M. Spatial and orientational distribution of cracks in crystalline photovoltaic modules generated by mechanical load tests. *Solar Energy Materials and Solar Cells* **2011**, *95*, 3054-3059.
196. Dallas, W.; Polupan, O.; Ostapenko, S. Resonance ultrasonic vibrations for crack detection in photovoltaic silicon wafers. *Measurement Science and Technology* **2007**, *18*, 852.
197. Belyaev, A.; Polupan, O.; Dallas, W.; Ostapenko, S.; Hess, D.; Wohlgemuth, J. Crack detection and analyses using resonance ultrasonic vibrations in full-size crystalline silicon wafers. *Applied Physics Letters* **2006**, *88*, 111907.
198. Hamid, S.A.; Zulkifli, M.N. Microstructure Evaluation of Photovoltaic Solar Panel's Interconnection: A Review. *Materials Science Forum* **2022**, *1055*, 27-35.
199. Rifat, A.; Pandao, P.P.; Babu, B.S. Solar Powered Fault Detection System for Railway Tracks. *European Journal of Electrical Engineering and Computer Science* **2022**, *6*, 39-43.
200. Pillai, D.S.; Rajasekar, N. Metaheuristic algorithms for PV parameter identification: A comprehensive review with an application to threshold setting for fault detection in PV systems. *Renewable and Sustainable Energy Reviews* **2018**, *82*, 3503-3525.
201. Chockalingam, A.; Naveen, S.; Sanjay, S.; Nanthakumar, J.; Praveenkumar, V. Sensor Based Hotspot Detection And Isolation In Solar Array System Using IOT. 2023; pp. 371-376.
202. Lee, H.-M.; Chae, W.-K.; Kim, W.-H.; Kim, J.-E. Cooperative Use of IMD and GPT in a 3-Phase Ungrounded Distribution System Linked to a Transformerless Photovoltaic Power Generation Facility. *Applied Sciences* **2023**, *13*, 1558.
203. Meribout, M.; Tiwari, V.K.; Herrera, J.P.P.; Baobaid, A.N.M.A. Solar panel inspection techniques and prospects. *Measurement* **2023**, 112466.
204. Garoudja, E.; Harrou, F.; Sun, Y.; Kara, K.; Chouder, A.; Silvestre, S. Statistical fault detection in photovoltaic systems. *Solar Energy* **2017**, *150*, 485-499.

205. Harrou, F.; Sun, Y.; Taghezouit, B.; Saidi, A.; Hamlati, M.-E. Reliable fault detection and diagnosis of photovoltaic systems based on statistical monitoring approaches. *Renewable energy* **2018**, *116*, 22-37.
206. Ali, M.H.; Rabhi, A.; El Hajjaji, A.; Tina, G.M. Real time fault detection in photovoltaic systems. *Energy Procedia* **2017**, *111*, 914-923.
207. Mustafa, Z.; Awad, A.S.A.; Azzouz, M.; Azab, A. Fault identification for photovoltaic systems using a multi-output deep learning approach. *Expert Systems with Applications* **2023**, *211*, 118551.
208. Lodhi, E.; Wang, F.-Y.; Xiong, G.; Zhu, L.; Tamir, T.S.; Rehman, W.U.; Khan, M.A. A Novel Deep Stack-Based Ensemble Learning Approach for Fault Detection and Classification in Photovoltaic Arrays. *Remote Sensing* **2023**, *15*, 1277.
209. Garoudja, E.; Chouder, A.; Kara, K.; Silvestre, S. An enhanced machine learning based approach for failures detection and diagnosis of PV systems. *Energy conversion and management* **2017**, *151*, 496-513.
210. Chen, L.; Li, S.; Wang, X. Quickest fault detection in photovoltaic systems. *IEEE Transactions on Smart Grid* **2016**, *9*, 1835-1847.
211. Chine, W.; Mellit, A.; Lughi, V.; Malek, A.; Sulligoi, G.; Pavan, A.M. A novel fault diagnosis technique for photovoltaic systems based on artificial neural networks. *Renewable Energy* **2016**, *90*, 501-512.
212. Et-taleby, A.; Chaibi, Y.; Benslimane, M.; Boussetta, M. Applications of Machine Learning Algorithms for Photovoltaic Fault Detection: a Review. *Statistics, Optimization & Information Computing* **2023**, *11*, 168-177.
213. Li, B.; Delpha, C.; Diallo, D.; Migan-Dubois, A. Application of Artificial Neural Networks to photovoltaic fault detection and diagnosis: A review. *Renewable and Sustainable Energy Reviews* **2021**, *138*, 110512.
214. Abubakar, A.; Almeida, C.F.M.; Gemignani, M. Review of artificial intelligence-based failure detection and diagnosis methods for solar photovoltaic systems. *Machines* **2021**, *9*, 328.
215. Kurukuru, V.S.B.; Haque, A.; Khan, M.A.; Sahoo, S.; Malik, A.; Blaabjerg, F. A review on artificial intelligence applications for grid-connected solar photovoltaic systems. *Energies* **2021**, *14*, 4690.
216. Tina, G.M.; Ventura, C.; Ferlito, S.; De Vito, S. A state-of-art-review on machine-learning based methods for PV. *Applied Sciences* **2021**, *11*, 7550.
217. Cotfas, D.T.; Cotfas, P.A.; Kaplanis, S. Methods to determine the dc parameters of solar cells: A critical review. *Renewable and Sustainable Energy Reviews* **2013**, *28*, 588-596.
218. Pan, J.-S.; Tian, A.-Q.; Pan, T.-S.; Chu, S.-C. Parameters Extraction of Solar Cell Using an Improved QUasi-Affine TRansformation Evolution (QUATRE) Algorithm. In *Advances in Intelligent Systems and Computing*; Springer: 2022; pp. 253-263.
219. Qin, J.; Wang, L.; Yang, S.; Huang, R. The effect of solar cell shunt resistance change on the bus voltage ripple in spacecraft power system. *Microelectronics Reliability* **2018**, *88*, 1047-1050.
220. d'Alessandro, V.; Guerriero, P.; Daliento, S.; Gargiulo, M. A straightforward method to extract the shunt resistance of photovoltaic cells from current–voltage characteristics of mounted arrays. *Solid-State Electronics* **2011**, *63*, 130-136.
221. Kim, Y.S.; Kang, S.-M.; Johnston, B.; Winston, R. A novel method to extract the series resistances of individual cells in a photovoltaic module. *Solar energy materials and solar cells* **2013**, *115*, 21-28.
222. Lucheng, Z.; Hui, S. Novel approach for characterizing the specific shunt resistance caused by the penetration of the front contact through the p–n junction in solar cell. *Journal of Semiconductors* **2009**, *30*, 074007.
223. Mohapatra, A.; Nayak, B.; Mohanty, K. Parameter Extraction of PV Module using NLS Algorithm with Experimental Validation. *International Journal of Electrical and Computer Engineering* **2017**, *7*, 2392.
224. Elyaqouti, M.; Saadaoui, D.; Lidaighbi, S.; Chaoufi, J.; Ibrahim, A.; Aqel, R.; Obukhov, S. A novel hybrid numerical with analytical approach for parameter extraction of photovoltaic modules. *Energy Conversion and Management: X* **2022**, *14*, 100219.
225. Meena, R.; Niyaz, H.M.; Gupta, R. Investigation and Differentiation of Degradation Modes Affecting Series Resistance in Photovoltaic Cells and Modules. *IEEE Journal of Photovoltaics* **2023**, *13*, 283-290, doi:10.1109/JPHOTOV.2023.3239744.
226. Ramalingam, K.; Indulkar, C.; Gharehpetian, G.B.; Mousavi Agah, S.M. Chapter 3 - Solar Energy and Photovoltaic Technology. In *Distributed Generation Systems*; Butterworth-Heinemann: 2017; pp. 69-147.
227. Roy, S.; Gupta, R. Quantitative Estimation of Shunt Resistance in Crystalline Silicon Photovoltaic Modules by Electroluminescence Imaging. *IEEE Journal of Photovoltaics* **2019**, *9*, 1741-1747, doi:10.1109/JPHOTOV.2019.2930402.

228. Kaplanis, S.; Kaplani, E. Energy performance and degradation over 20 years performance of BP c-Si PV modules. *Simulation Modelling Practice and Theory* **2011**, *19*, 1201-1211.
229. Dhass, A.D.; Beemkumar, N.; Harikrishnan, S.; Ali, H.M. A Review on Factors Influencing the Mismatch Losses in Solar Photovoltaic System. *International Journal of Photoenergy* **2022**, *2022*.
230. Sinha, A.; Sastry, O.; Gupta, R. Nondestructive characterization of encapsulant discoloration effects in crystalline-silicon PV modules. *Solar Energy Materials and Solar Cells* **2016**, *155*, 234-242.
231. Lin, L.; Bora, B.; Prasad, B. Influence of outdoor conditions on PV module performance–an overview. *Material Sci & Eng* **2023**, *7*, 88-101.
232. Pavlík, M.; Beňa, L.u.; Medved', D.; Čonka, Z.; Kolcun, M. Analysis and evaluation of photovoltaic cell defects and their impact on electricity generation. *Energies* **2023**, *16*, 2576.
233. Gxasheka, A.R.; Van Dyk, E.E.; Meyer, E.L. Evaluation of performance parameters of PV modules deployed outdoors. *Renewable Energy* **2005**, *30*, 611-620.
234. Rajput, P.; Malvoni, M.; Kumar, N.M.; Sastry, O.S.; Tiwari, G.N. Risk priority number for understanding the severity of photovoltaic failure modes and their impacts on performance degradation. *Case Studies in Thermal Engineering* **2019**, *16*, doi:10.1016/j.csite.2019.100563.
235. Sinha, A.; Sastry, O.S.; Gupta, R. Nondestructive characterization of encapsulant discoloration effects in crystalline-silicon PV modules. *Solar Energy Materials and Solar Cells* **2016**, *155*, 234-242.
236. Al Mahdi, H.A.; Leahy, P.G.; Morrison, A.P. Predicting Early EVA Degradation in Photovoltaic Modules From Short Circuit Current Measurements. *IEEE Journal of Photovoltaics* **2021**.
237. Ruschel, C.S.; Gasparin, F.P.; Costa, E.R.; Krenzinger, A. Assessment of PV modules shunt resistance dependence on solar irradiance. *Solar Energy* **2016**, *133*, 35-43.
238. Zhang, J.; Liu, Y.; Ding, K.; Feng, L.; Hamelmann, F.U.; Chen, X. Model Parameter Analysis of Cracked Photovoltaic Module under Outdoor Conditions. *2020 47th IEEE Photovoltaic Specialists Conference (PVSC)* **2020**, 2509-2512.
239. Oh, J.; Bowden, S.; TamizhMani, G. Potential-induced degradation (PID): Incomplete recovery of shunt resistance and quantum efficiency losses. *IEEE Journal of Photovoltaics* **2015**, *5*, 1540-1548.
240. Luo, W.; Khoo, Y.S.; Hacke, P.; Naumann, V.; Lausch, D.; Harvey, S.P.; Singh, J.P.; Chai, J.; Wang, Y.; Aberle, A.G. Potential-induced degradation in photovoltaic modules: a critical review. *Energy & environmental science* **2017**, *10*, 43-68.
241. Hacke, P.; Spataru, S.; Johnston, S.; Terwilliger, K.; VanSant, K.; Kempe, M.; Wohlgemuth, J.; Kurtz, S.; Olsson, A.; Propst, M. Elucidating PID Degradation Mechanisms and In Situ Dark I–V Monitoring for Modeling Degradation Rate in CdTe Thin-Film Modules. *IEEE Journal of Photovoltaics* **2016**, *6*, 1635-1640, doi:10.1109/JPHOTOV.2016.2598269.
242. Dhass, A.D.; Natarajan, E.; Ponnusamy, L. Influence of shunt resistance on the performance of solar photovoltaic cell. *2012 International Conference on Emerging Trends in Electrical Engineering and Energy Management (ICETEEEM)* **2012**, 382-386.
243. van Dyk, E.E.; Meyer, E.L. Analysis of the effect of parasitic resistances on the performance of photovoltaic modules. *Renewable Energy* **2004**, *29*, 333-344, doi:https://doi.org/10.1016/S0960-1481(03)00250-7.
244. Sarkar, M.N.I. Effect of various model parameters on solar photovoltaic cell simulation: a SPICE analysis. *Renewables: Wind, Water, and Solar* **2016**, *3*, 1-9.
245. Kennerud, K.L. Analysis of performance degradation in CdS solar cells. *IEEE Transactions on aerospace and electronic systems* **1969**, 912-917.
246. Rummel, S.R.; McMahon, T.J. Effect of cell shunt resistance on PV module performance at reduced light levels. *AIP conference proceedings* **1996**, *353*, 581-586.
247. Al Mahdi, H. Predicting photovoltaic module degradation using current-voltage. **2022**.
248. Hussain, T.; Hussain, M.; Al-Aqrabi, H.; Alsboui, T.; Hill, R. A Review on Defect Detection of Electroluminescence-Based Photovoltaic Cell Surface Images Using Computer Vision. *Energies* **2023**, *16*, 4012.
249. Zamzeer, A.S.; Farhan, M.S.; Rikabi, H.T.S.A. An Investigation into Faults of PV system using Machine Learning: A Systematic Review. In Proceedings of the 2023 Third International Conference on Advances in Electrical, Computing, Communication and Sustainable Technologies (ICAECT), 5-6 Jan. 2023, 2023; pp. 1-6.

250. Mansouri, M.; Trabelsi, M.; Nounou, H.; Nounou, M. Deep Learning-Based Fault Diagnosis of Photovoltaic Systems: A Comprehensive Review and Enhancement Prospects. *IEEE Access* **2021**, *9*, 126286-126306, doi:10.1109/ACCESS.2021.3110947.
251. Zeb, K.; Islam, S.U.; Khan, I.; Uddin, W.; Ishfaq, M.; Curi Busarello, T.D.; Muyeen, S.M.; Ahmad, I.; Kim, H.J. Faults and Fault Ride Through strategies for grid-connected photovoltaic system: A comprehensive review. *Renewable and Sustainable Energy Reviews* **2022**, *158*, 112125, doi:https://doi.org/10.1016/j.rser.2022.112125.